The Republic of the Union of Myanmar

Ministry of Natural Resources and Environmental Conservation

Environmental Conservation Department

ESTIMATION OF HIGH SPATIAL AND TEMPORAL RESOLUTION OF $PM_{2.5}$ CONCENTRATIONS IN CHIANG MAI USING SATELLITE-DERIVED AEROSOL OPTICAL DEPTHS AND METEOROLOGICAL PARAMETERS

Pyae Phyo Kyaw
Staff Officer
Environmental Conservation Department
Shan State

ကောင်းကင် ဂြိုလ်တုမှ ရရှိသည့် လေထုအတွင်းရှိ အမှုန်အမွှားပါဝင်မှု အချက်အလက်များနှင့် မိုးလေဝသ ဆိုင်ရာအချက်အလက်များ အသုံးပြု၍ ချင်းမိုင်ဒေသအတွင်း နေရာနှင့်အချိန်ပုံရိပ်ပြတ်သားမှု မြင့်မားစွာဖြင့် PM2.5 ပမာဏအား ခန့်မှန်းတွက်ချက်ခြင်း

လေထုအတွင်း သာမန် မျက်စိဖြင့် မမြင်နိုင်သော အလွန်သေးငယ်သည့် အမှုန်အမွှား များ(Particulate Matter-PM) ညစ်ညမ်းမှုကြောင့် ကမ္ဘာတစ်ဝှမ်းတွင် နှစ်စဉ်လူဦးရေ(၄.၂) မီလီယံခန့်သေဆုံးလျက်ရှိကြောင်း ကမ္ဘာ့ကျန်းမာရေးအဖွဲ့အစည်းWorld Health Organization-WHO ၏ အစီရင်ခံစာ(၂၀၂၁) တွင် ဖော်ပြထားပြီး လေထုညစ်ညမ်းမှု လျော့ချရေးလုပ်ငန်း များအား ထိရောက်စွာ အကောင်အထည်ဖော် ဆောင်ရွက်ရန် လိုအပ်ကြောင်းနှင့် အများစုသော ဖွံ့ဖြိုးဆဲနိုင်ငံများ၏ လေထုအရည်အသွေးမှာ WHO ၏ သတ်မှတ်တန်ဖိုးများအောက် ရောက်ရှိ နေကြောင်းဖော်ပြထားပါသည်။ လေထု ညစ်ညမ်းစေသည့် အရာများအမျိုးမျိုးရှိသည့် အနက် သာမန် မျက်စိဖြင့်မမြင်နိုင်သည့် အလွန်သေးငယ်သည့် အမှုန်အမွှားများ (PM2.5) ကြောင့် လူသားတို့၏ ကျန်းမာရေး ထိခိုက်မှုမှာ နှစ်စဉ်မြင့်တက်လျက်ရှိပြီး အဓိကအားဖြင့် အသက်ရှူ လမ်းကြောင်း ဆိုင်ရာရောဂါများ၊ နှလုံးရောဂါများ၊ ကင်ဆာရောဂါများ ဖြစ်ပွားစေ နိုင်ပါသည်။ လေထု ညစ်ညမ်းမှုထိန်းချုပ်ရေး စီမံခန့်ခွဲမှု လုပ်ငန်းများအား ထိရောက်စွာ ဆောင်ရွက်ရန် လိုအပ်ပြီး လေထုအရည်သွေး စောင့်ကြည့်တိုင်းတာခြင်း လုပ်ငန်းမှာလည်း အဓိကအခန်းမှ ပါဝင်ပါသည်။ လေထုအရည်အသွေး အခြေအနေအား သိရှိမှသာလျှင် လျော့ချရေးလုပ်ငန်းများ ထိရောက်စွာ ဆောင်ရွက်နိုင်မည်ဖြစ်ပါသည်။

မြေပြင်လေထုအရည်အသွေး စောင့်ကြည့်ခြင်းလုပ်ငန်းများ ဆောင်ရွက်ရာတွင် လေထု အရည်အသွေးစောင့်ကြည့်ရေး စက်ကိရိယာများနှင့် စနစ်များ တပ်ဆင် ရေးလုပ်ငန်းများမှာ ငွေကြေးသုံးစွဲရမှု မြင့်မားခြင်းကြောင့် ဖွံ့ဖြိုးဆဲနိုင်ငံများ အတွက် လုံလောက်သည့် Air Quality Monitoring Network မှာ အားနည်းလျက် ရှိပါသည်။ ဖွံ့ဖြိုးပြီးနိုင်ငံများတွင် လေထုအရည် အသွေးစောင့်ကြည့်ရေး စနစ်များ လုံလောက်စွာ တပ်ဆင်နိုင် သောကြောင့် လေထုညစ်ညမ်းမှု ထိန်းချုပ်ရေးလုပ်ငန်းများအား အောင်မြင် ထိရောက်စွာ ဆောင်ရွက်နိုင်ပြီဖြစ်ပါသည်။

ယခုအခါ မြေပြင်တွင် လေထုအရည်အသွေးတိုင်းတာစောင့်ကြည့်ရေးစနစ်များ မရှိ သည့် နေရာများတွင် ကောင်းကင်ဂြိုဟ်တုများမှ Remote Sensing System ဖြင့် ရရှိသည့် လေထုအတွင်း အမှုန်ပါဝင်မှု (Aerosol Optical Depths-AOD) နှင့် မိုးလေဝသဆိုင်ရာ အတိုင်းအတာများ (Meteorological Parameters)အား အသုံးပြု၍ နေရာဒေသတစ်ခု၏ လေထု အရည်အသွေးအခြေအနေအား အနီးစပ်ဆုံးခန့်မှန်းခြင်း လုပ်ငန်းများ ဆောင်ရွက်နိုင်ပြီ ဖြစ်ပါ သည်။

စာတမ်းပြုစုနိုင်ရေးအတွက် Study Area ရွေးချယ်ခြင်း ဆောင်ရွက်ရာတွင် မြန်မာ နိုင်ငံနှင့် နယ်နိမိတ်ချင်းထိစပ်နေပြီး နှစ်စဉ် ပွင့်လင်းရာသီ၌ လေထုညစ်ညမ်းမှုဆိုးရွားစွာ ဖြစ်ပေါ်လေ့ရှိသည့် ချင်းမိုင်ဒေသအား ရွေးချယ်ခဲ့ပါသည်။ ချင်းမိုင်ဒေသတွင်ရှိသည့် လေထု အရည်အသွေးစောင့်ကြည့်တိုင်းတာသည့်နေရာ (၂) နေရာနှင့် မိုးလေဝသ အချက်အလက်များ တိုင်းတာသည့် နေရာ(၂)နေရာ စုစုပေါင်း (၄) နေရာမှ PM2.5, Temperature, Relative Humidity, Wind Speed, Wind direction စသည့် လေထုအရည်အသွေး ဆိုင်ရာအချက် အလက်များအား ထိုင်းနိုင်ငံ၊ ပတ်ဝန်းကျင် ညစ်ညမ်းမှု ထိန်းချုပ်ရေးဌာနမှ တောင်းခံရရှိ ပါသည်။ အချက်အလက်များမှ ၂၀၂၀ ခုနှစ်အတွင်း နေ့စဉ်တိုင်းတာရရှိသည့် လေထုအရည် အသွေးရလဒ်များ အား သုတေသနအတွက် အသုံးပြုခဲ့ပြီး ကောင်းကင်ဂြိုလ်တုမှ လိုအပ်သည့် အချက်အလက် များအား NASA Earth Data ၏ Moderate Resolution Imaging Spectroradiometer(MODIS) နှင့် Japan Meteorological Center ၏ Himawari-8 Satellite မှ ၂၀၂၀ ခုနှစ်အတွင်း လိုအပ်သည့် နှစ်အလိုက် နေ့စဉ်ရရှိခဲ့သည့် Data များအား တောင်းခံ၍ သုတေသနတွင် အသုံးပြုခဲ့ပါသည်။ရရှိသည့် မြေပြင် PM2.5 ပမာဏ အချက်အလက်များနှင့် ဂြိုလ်တုမှ Aerosol Optical Depth အချက်အလက် များ၏ ဆက်နွယ်မှုအား Data Analysis, Multiple Linear Regression method ဖြင့် ဖော်ထုတ်ရာတွင် positive relationship ရရှိခဲ့ပြီး ဆက်နွယ်မှုမှာ ၇၀ ရာခိုင်နှုန်း ခန့်ရှိကြောင်း တွေ့ရှိခဲ့ရပါသည်။

သုတေသနတွေ့ရှိချက်အရ PM2.5 ပမာဏအနေဖြင့် ပွင့်လင်းရာသီဖြစ်သည့် ဒီဇင်ဘာလ မှ ဧပြီလအတွင်း မြင့်မားကြောင်းနှင့် ကျန်ကာလများတွင် ပမာဏလျော့နည်း ကြောင်းတွေ့ရှိ ရပါသည်။ ကောင်းကင်ဂြိုလ်တုမှ ရရှိသည့် လေထုအတွင်းအမှုန်ပါဝင်မှု အချက်အလက်များ မှာ မိုးရာသီကာလ တိမ်ထူထပ်သည့် နေ့ရက်များတွင် ရရှိနိုင်မှု မရှိကြောင်း တွေ့ရှိရပါသည်။ PM2.5 ပမာဏမှာ နံနက်ပိုင်းအချိန်ဖြစ်သည့် နံနက် ၉:၀၀

နာရီမှ နေ့လည် ၁:၀၀ အတွင်း မြင့်မားကြောင်းတွေ့ရှိရပါသည်။ ချင်းမိုင်ဒေသသည် ထိုင်းနိုင်ငံ၏ မြောက်ပိုင်းတွင်တည်ရှိပြီး အဓိကအားဖြင့် စိုက်ပျိုးရေးလုပ်ငန်းများ ဆောင်ရွက်ကြပြီး နှစ်စဉ်ပွင့်လင်းရာသီတွင် စိုက်ပျိုး ရေးလုပ်ငန်းအကြွင်းအကျန်များ မီးရှို့ခြင်း၊ တောမီးလောင်ခြင်းများကြောင့် PM2.5 ပမာဏများ ပြားစွာထွက်ရှိပြီး လေထုညစ်ညမ်းမှုဖြစ်ပေါ်လေ့ရှိပါသည်။ ချင်းမိုင်ဒေသသည် တောင်တန်း ထူထပ်သည့်ဒေသဖြစ်ပြီး အပူပိုင်းသမရာသီဥတုရှိသောဒေသဖြစ်ပါသည်။ PM2.5 ပမာဏမှာ မိုးလေဝသဆိုင်ရာ အချက်အလက်များဖြစ်သည့် လေထုအပူချိန်နှင့် စိုထိုင်းစ၊ လေတိုက်ခတ်ရာ လမ်းကြောင်းနှင့် လေတိုက်နှုန်းများအပေါ် မူတည်၍ ပျံ့နှံ့မှုများ ကွဲပြားကြောင်း တွေ့ရှိရပါသည်။ ချင်းမိုင်ဒေသအနေဖြင့် နှစ်စဉ် ပွင့်လင်းရာသီကာလများ အတွင်း လေထုညစ်ညမ်းမှု ဖြစ်ပေါ်လေ့ရှိပြီး PM2.5 ပမာဏမှာ 80 µg/m3 အထက်သို့ရောက်ရှိကြောင်း၊ တောမီးလောင်ခြင်း၊ တောင်ယာမီးရှို့ခြင်းများကြောင့် နယ်စပ် ဖြတ်ကျော်မီးခိုးမြူငွေ့ညစ်ညမ်းမှုများဖြစ်ပေါ် လေ့ရှိကြောင်းတွေ့ရှိရပါသည်။

Abstracts

Particulate Matter (PM) is one of the most common pollutants emitted from anthropogenic sources because they can be formed from the numerous types of sources. Chiang Mai faces high level of $PM_{2.5}$ concentration during dry season of every year. To monitor $PM_{2.5}$ condition, there are only two air quality monitoring stations in Chiang Mai. Insufficient monitoring stations makes the limitation in air quality management. Nowadays, satellite remote sensing become a tool to monitor air pollutants on the earth surface where there are not enough monitoring stations. Aerosol Optical Depth (AOD) is one of the parameters to show the condition of air quality in the atmosphere. There are many different satellites that provide AOD products with different temporal and spatial resolution.

In this study, AOD from MAIAC, having 1x1 km^2 spatial resolution and AOD from Himawari-8 satellite having 5x5 km^2 spatial resolution, were used to develop hourly 1x1 km^2 resolution AOD to estimate $PM_{2.5}$ concentration in Chiang Mai for the year 2020. These AOD were validated with the ground-based AOD from Chiang Mai AERONET station, and the result showed a correlation coefficient (R^2) of 0.63. This hourly high-resolution AOD data was used to estimate $PM_{2.5}$ concentration by using Multiple Linear Regression with 1-hr average ground-based $PM_{2.5}$ concentration data from the monitoring stations. The results showed that the R^2 was 0.56 for the relationship between AOD and $PM_{2.5}$ only. The meteorological parameters, i.e., temperature, relative humidity, wind speed, and wind direction were added in the model, and the R^2 was improved to 0.62. Random Forest Regression was also applied to compare the results of correlation, and the R square results were 0.95 in the training set and 0.53 in the testing set. This regression showed the most important variable was aerosol optical depth in estimation of $PM_{2.5}$.

The estimated $PM_{2.5}$ concentrations were correlated with the observed $PM_{2.5}$ with an R^2 of 0.71. The mean bias was 1.115 and the root mean squared error was 23.28 $\mu g/m^3$. The correlation results of different hours from 09:00 to 16:00 hr. varied from 0.55 at 14:00 hr. to 0.81 at 10:00 hr. Finally, the hourly spatial distribution maps of $PM_{2.5}$ concentration over Chiang Mai were developed with the relationship between hourly 1x1km^2 spatial resolution AOD and $PM_{2.5}$ with meteorological parameters.

Table of Contents

List of Tables

List of Figures

Figure	Title	Page

List of Abbreviations

AERONET	Aerosol Robotic Network
AHI	Advanced Himawari Image
AOD	Aerosol Optical Depth
AQI	Air Quality Index
BMR	Bangkok Metropolitan Region
EM	Electromagnetic
EOS	Earth Observing System
GOES	Geostationary Operational Environmental Satellite
IDW	Inverse Distance Weight
JMA	Japan Meteorological Agency
LR	Linear Regression
MAE	Mean Square Error
MAIAC	Multi-Angle Implementation of Atmospheric Correction
MLR	Multiple Linear Regression
MODIS	Moderate Resolution Imaging Radiometer
NAAQS	National Ambient Air Quality Standards
NASA	National Aeronautics and Space Administration
PCD	Pollution Control Department
PHOTONS	Physic, Optoelectronics, and Technology of Novel Micro-resonator Structures
PM	Particulate Matter
RFR	Random Forest Regression
RH	Relative Humidity
RSME	Root Mean Square Error
SPSS	Statistical Package for the Social Sciences
SSA	Single Scattering Albedo
TMD	Thailand Meteorological Department

Chapter 1

Introduction

1.1 Background

With an increasing in global population and anthropogenic activity, many types of environmental pollutions are threatening our environment. From past to present, the composition of atmosphere has become more polluted due to natural events and anthropogenic activities. Air pollution is one of the greatest environmental risk to health, accounting for seven million deaths around the world every year (WHO, 2021). Different types of air pollutants are being emitted into our atmosphere. Among all of these air pollutants, Particulate Matter (PM) is the most common one because they can be generated from the various types of sources. PM with diameters smaller than or equal to 10 µm (PM_{10}) and 2.5µm ($PM_{2.5}$) are considered as coarse and fine particles, respectively. Fine particles can be easily transported over long distances on the current of air in atmosphere and may be drawn into the respiratory airways of human causing adverse health effects (Lim S. et al., 2009). In order to control and manage $PM_{2.5}$ pollution, it is important to know the sources of pollutants and their characteristics, such as their dispersion, accumulation and effects to receptors (Dayou et al., 2014).

Effective management system for air pollution problems needs accurate data related to the condition and concentration of air pollutants. Monitoring is one of the most effective tools for air quality management. Many air quality monitoring technologies and equipment are widely used especially in developed countries. Most developing countries, on the other hand, have limitations to install ground-based monitoring stations. In Thailand, Pollution Control Department (PCD) has established a network to monitor air pollution with monitoring stations (Jansakoo, 2020). With the limitation of cost and technology, air quality monitoring stations cannot be installed to get the sufficient air quality data for the whole area. To fulfill this gap, monitoring by satellite data become one solution with valuable result (Bhaskaran et al., 2011).

Remote sensing has been widely used for environmental application, such as air and water qualities monitoring (Lim S. et al., 2009). Estimations of the condition of air pollutants by using remote sensing and satellite images become the effective tool in air quality monitoring. With broad spatial coverage, satellite data can potentially expand ground monitoring networks for air quality estimation. Satellite sensors such as Moderate Resolution Imaging Spectroradiometer (MODIS) and Hamawari-8 satellite generate Aerosol Optical Depth (AOD).

MODIS is an imaging sensor of the NASA satellites that was launched into Earth Obit in 1999 and 2002. MODIS provide measurements in large scale global dynamic including changes in the Earth's atmosphere, ocean and land with 36 spectral bands ranging in wavelength from 0.4m to 14.4m and at varying spatial resolution 250m to 1000m. However, MODIS can only provide AOD data in any location at two times per day. Another satellite is Hamawari-8 which is geostationary weather satellite operated by Japan Meteorological Agency. This satellite has 16 spectral band to capture the visible light and infrared images. Hamawari-8 can provide AOD data for every 10-minute interval with the spatial resolution of 5 x 5 km^2.(LAADS DAAC, 2020)

Air pollution is a significant problem in the northern part of Thailand every year, particularly during the dry season from December to April. Particulate matter from transportation, industrial, and residential sectors, open burning of agricultural residues, and forest fires are the major sources of air pollution. In northern Thailand, the agricultural sector is the primary source of air pollution. Chiang Mai province is the second largest province of Thailand and located in upper northern Thailand. Chiang Mai is very famous in tourism with many beautiful natures such as mountains, hill and tribes' villages. However, Chiang Mai province usually faces $PM_{2.5}$ concentration problem during dry and cold season of every year due to emission from anthropogenetic activities, especially agricultural open burning after harvesting period and bad meteorological condition (IQAir, 2020). Currently, there are only two permanent air quality monitoring stations in Chiang Mai. These monitoring stations cannot cover and represent the air quality status of the whole province. In this study, hourly $PM_{2.5}$ concentration were estimated and compared with the ground-based $PM_{2.5}$ data using AOD from the satellites.

1.2 Statement of Problem

In Thailand, AOD from satellites images has been widely used to monitor ground-based $PM_{2.5}$ concentrations because of insufficient air quality monitoring stations. However, there are still remaining factors to get high accuracy air quality data with the coarse spatial and temporal resolutions of the satellite AOD products which have the weakness to capture the characteristics of $PM_{2.5}$ in the city which change rapidly. Jansakoo (2020) has developed the AOD from MODIS with the resolution of 500x500 m^2 over Bangkok Metropolitan Region (BMR) which is finer than the normal resolution used elsewhere in Thailand. However, the MODIS satellite passes over Thailand just two times per day, and it cannot provide hourly $PM_{2.5}$ concentration prediction. Moreover, another satellite known as Hamawari-8 which can provide hourly AOD was used to estimate the hourly $PM_{2.5}$ concentration for Chiang Mai (Samermit, 2020), but this also had a different limitation for $PM_{2.5}$ prediction with the rough spatial resolution of the AOD product (5000x5000 m^2) which is unable to be related to the urban landscape or small geographical units. The main problem needed to be addressed is that the development of high resolution in both spatial and temporal distribution for the estimation of $PM_{2.5}$ concentrations using the combination of the products from MODIS and Himawari-8 satellites.

1.3 Objectives

The overall objective of this study is to develop hourly high spatial resolution of $PM_{2.5}$ concentration in Chiang Mai by using ground-based air quality monitoring data and AOD products of MODIS with Multi-Angle Implementation of Atmospheric Correction (MAIAC) and Hamawari-8 satellites. The specific objectives of this study are:

- To develop the hourly 1x1 km^2 of AOD data from MODIS-MAIAC and Himawari-8 satellite for Chiang Mai province.
- To estimate $PM_{2.5}$ concentration from the AOD products and meteorological parameters using statistical analysis and machine learning approach.

1.4 Scope of the Study

This study focused on $PM_{2.5}$ concentration and the Aerosol Optical Depth products from MAIAC from MODIS sensors and Hamawari-8 sensor for the year of 2020. Chiang Mai province was selected as a study area that located in the northmost part of Thailand because this area is usually faced air pollution every year and has very limitation of air monitoring stations. Hourly ground-based monitoring data of $PM_{2.5}$ concentration was collected from the air quality monitoring stations in Chiang Mai. Meteorological factors that can influent the concentration and dispersion of air pollutants were considered to get the higher model performance in this study.

Chapter 2

Literature Review

2.1 Study Area

Thailand is situated in the central of Southeast Asia's mainland. Thailand occupies a land area of around 513,000 square kilometers and is shaped like an axe. The northern portion of the country shares borders with Myanmar, Laos, and Cambodia, while the southern portion shares borders with Malaysia and the Gulf of Thailand. It is divided into four natural regions: the North, the Central Plain or the Chao Phraya River Basin, the Northeast or the Korat Plateau, and the South or the Southern Peninsula. Thailand's weather conditions are influenced by the Monsoon of South-West and the North-East. Seasons are classified as winter, summer, and rainy. Thailand is divided into 77 provinces, each of which is divided into smaller districts. Chiang Mai is one of these provinces, located in northern Thailand. The study focuses on Chiang Mai Province, which is the largest province in northern Thailand.

2.1.1 Background

Chiang Mai Province, the second largest province in Thailand, is located the northern part of the Thailand and 685 kilometers north from Bangkok. It is surrounded by the mountain ranges of Thai highlands on average at 1000 ft elevation with tropical wet and dry climate. Total area of Chiang Mai province is approximately 20,107 km^2 with an approximately 1.7 million of population (National Statistical Office, 2019). Chiang Mai city is the capital of province and one of the most tourist attractive provinces in Thailand due to its beautiful mountain ranges, valleys, and cultural heritages. Chiang Mai Province is divided into 25 districts and nearly 80% of the province area are hilly regions. Major land-use type in Chiang Mai is Agricultural area and it covers 45.5 % of the whole province. Figure (2.1) and (2.2) show the location and Land used type of Chiang Mai Province.

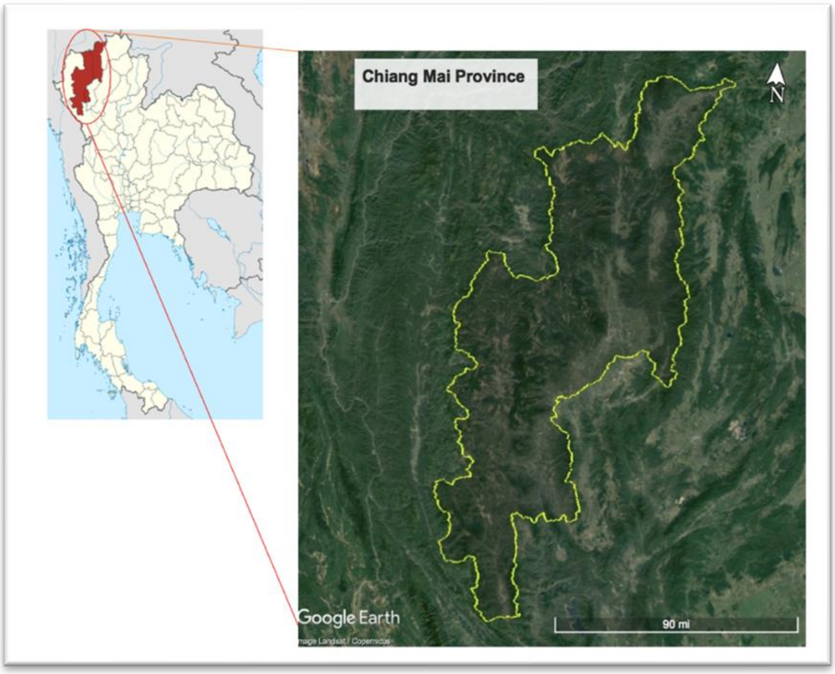

Figure 2.1: Location of Study Area, Chiang Mai Province

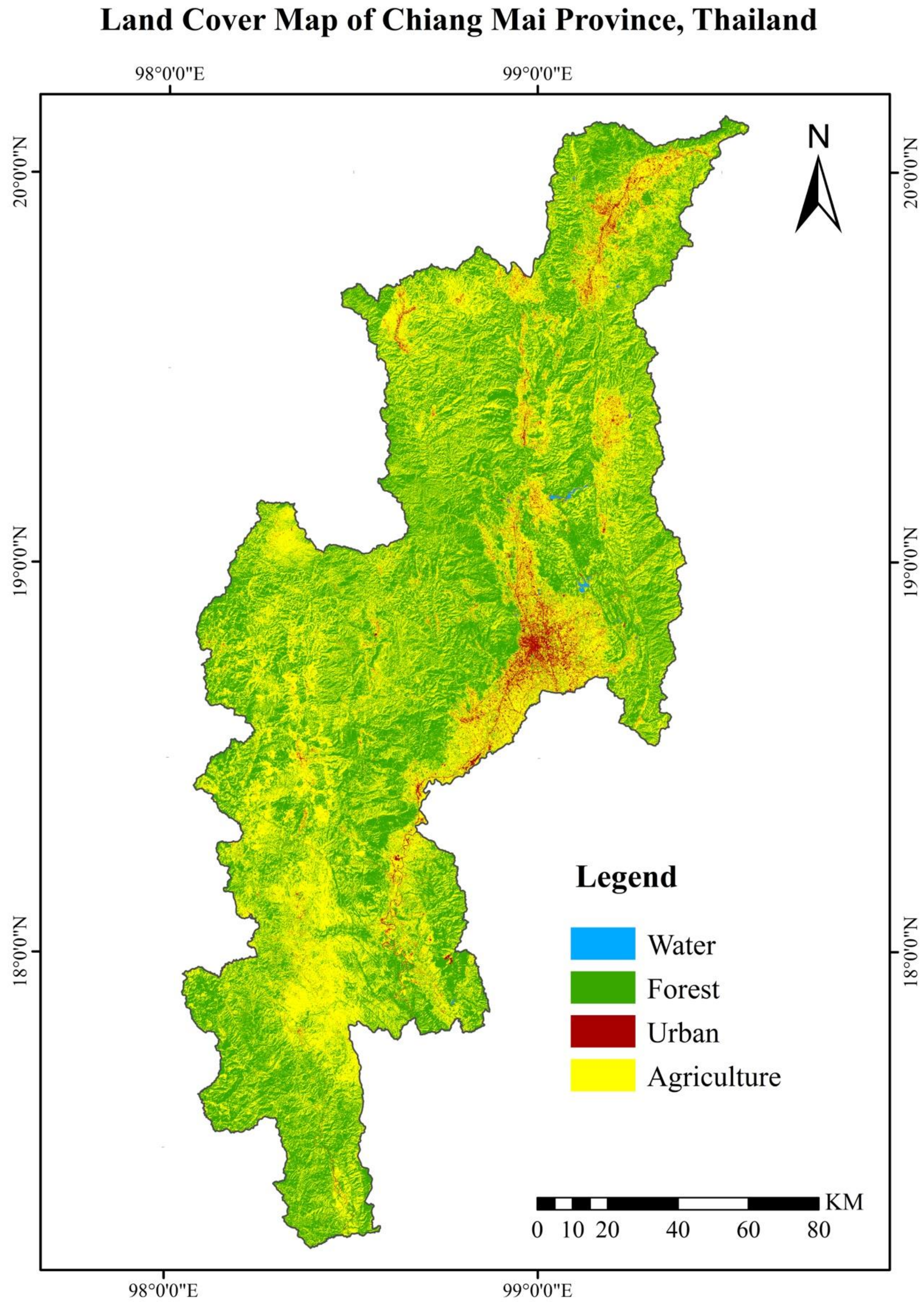

Figure 2.2: Major Land cover Map of Chiang Mai Province (USGS, 2021)

2.1.2 Air Quality in Chiang Mai

Chiang Mai is located in upper northern Thailand, a region prone to weather variations as a result of its geographic location. Chiang Mai usually suffers from air pollution concerns, particularly during the dry season, due to its diverse weather conditions and agricultural activities. Over the last decade, Chiang Mai has faced with air pollution, particularly $PM_{2.5}$ pollution. During the dry season, PM concentrations typically exceed the national air quality limit, and Chiang Mai is listed as the highest PM pollution region in the country. Each year, the number of days where PM_{10} levels above national guidelines varied between 30% and 40% of the monitoring days during the haze season (PCD, 2015). Open burning of biomass during the dry season in northern Thailand and neighboring countries is the primary source of high $PM_{2.5}$ concentrations in Chiang Mai. Chiang Mai's air pollution sources include traffic conditions, industry, home waste burning, agricultural burning, and forest fires. PM pollution can cause environmental and health issues such as respiratory problems. $PM_{2.5}$ has a detrimental effect on the respiratory system, entering deeply into the lung and causing cancer.

The major emission source in Chiang Mai is agricultural biomass open burning during dry season. Another important factor affecting regional air quality is the topographical landscape, which is complicated and characterized by valleys, particularly in hilly locations. Chiang Mai usually face haze pollution during harvesting period of every year due to open burning of crops, forest fire, dry weather condition, and transboundary air pollutants from bounder countries. Haze is an atmospheric phenomenon in which dust, smoke and other particulate matter obstruct visual clarity. In Chiang Mai, haze pollution is observed between November and February. Thailand usually faces transboundary haze pollution in the northern region from Myanmar and in the southern region from Indonesia. The period From February to April is the highest pollution level and the air quality is increasing back after April. "Pollution Control Department of Thailand (PCD) has installed an air quality monitoring network with the objective of providing continuous atmospheric parameters such as particulate matter (PM), Sulfur dioxide (SO_2), Carbon dioxide (CO), Nitrogen dioxide (NO_2) and some meteorological data also."

There are two ground-based air quality monitoring station in Chiang Mai Province which are Chiang Mai City Hall station 35T located at the Chang Phueak, Meuang, and Yupparaj Witthayalai station 36T located at Si Phum, Meuang, Chiang Mai Province. In 2019, PCD also provided four mobile air quality monitoring stations in order to access more information about the air pollution status in Chiang Mai Province.

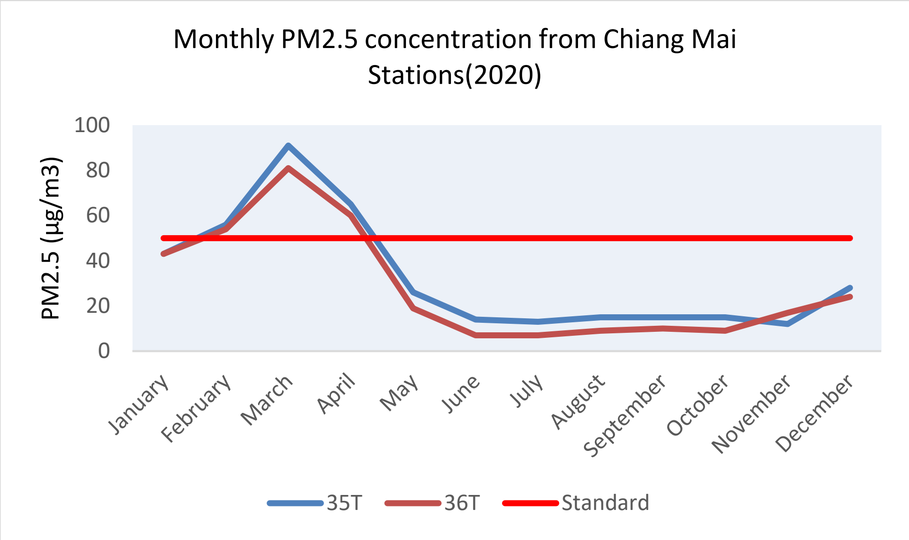

Figure 2.3: $PM_{2.5}$ concentrations of Station 35T and 36T in Chiang Mai for 2020 (PCD Thailand)

2.2 Particulate Matter

Particulate matter (PM) is a term referring to a mixture of particles and liquid found in the air. Particulate matter is composed of a variety of substances, including black carbon, organic carbon, trace metals, crustal material, and so on. They vary in size and composition according to geographical region and time period. Some particles, such as dust and dirt, are visible to the naked eye, while others are extremely minute and can only be detected under a microscope. They are the primary contributors of air pollution. PM emissions originate from either human-caused or natural sources. They are generated in the atmosphere as a result of the combustion of a sequence of gaseous by-products. $PM_{2.5}$ has the greatest health impact of all air pollution metrics. $PM_{2.5}$ can remain in the atmosphere for long time due to its small size and can be absorbed deeply into the circulation by inhalation.

2.2.1 Types of Particulate Matters

Particulate matters can be divided as Primary and Secondary PM according to their formation and nature. Primary PM are emitted from combustion processes and mechanical disruption processes and man- or wind-induced events causing suspension of particles. Secondary PM is formed by gas-to-particle conversion in the atmosphere and/or condensation of gaseous compounds. Commonly, there are two main groups divided by different sizes. PM with diameter less than or equal to 10 µm are called as (PM_{10}) and less than or equal to 2.5 µm called ($PM_{2.5}$), also known as fine particles. Ultrafine particles which have less than 0.1 microns in diameter are known as airborne particles and they represent more than 90% of all airborne pollutants (IQAir,2021). They causes human health problems especially in brain, lungs, throat, eyes, heart, and so on.Figure (2.3) illustrate the size of PM with different Types.

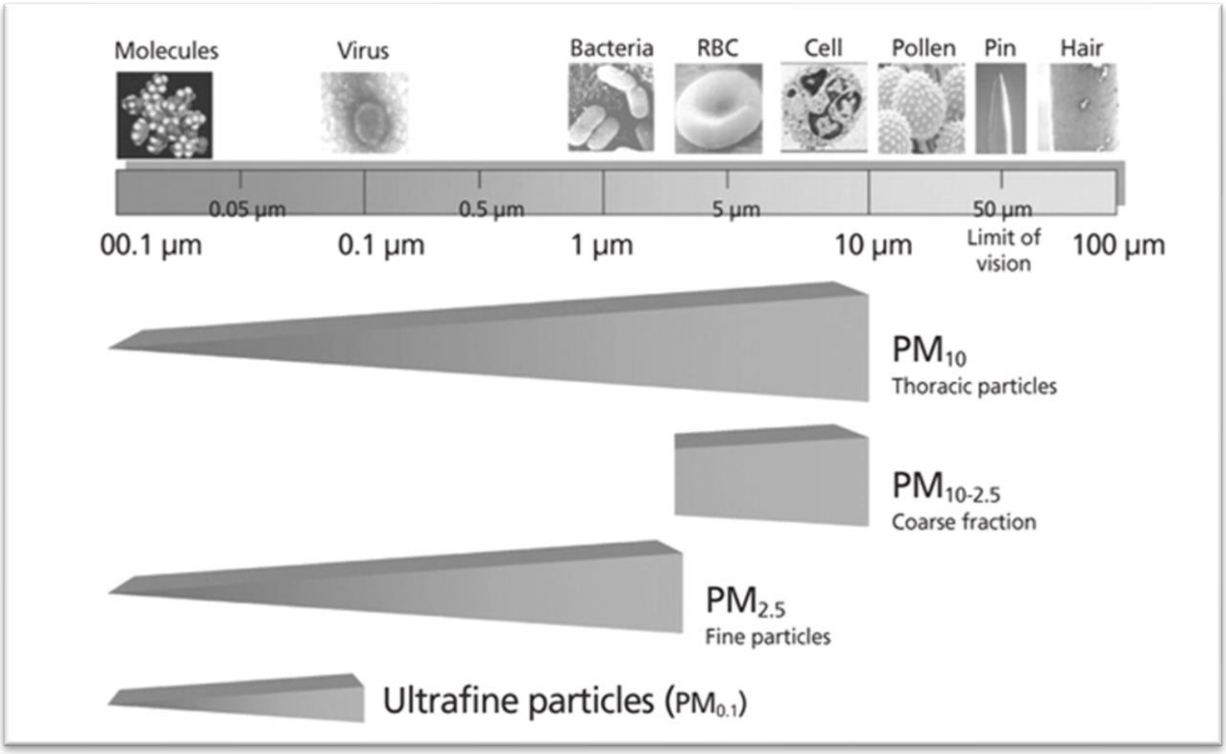

Figure 2.4: Different size and types of Particulate Matters

2.2.2 Sources of $PM_{2.5}$

Particulate Matters ($PM_{2.5}$) can be generated from both natural processes and anthropogenic activities. Natural event is the major source of PM in the ambient air. These include volcanic eruption, pollen, windblown dust and forest fires. Although anthropogenic sector constitutes less contribution, it can significantly emit and generate to decrease the air quality downwind of urban and industrial areas. Man-made activities include agricultural operations, industrial processes, combustion of wood and fossil fuels, construction, mining, smoking and entrainment of road dust into the air. $PM_{2.5}$ sources vary with season, weather, climate, urbanization level, country, and location, and may also include emissions from neighboring countries. $PM_{2.5}$ can be generated from chemical reaction with other pollutants in the atmosphere. Chemical reactions with sulfur dioxide, nitrogen oxides, and VOCs are also sources of $PM_{2.5}$ pollutants.

2.2.3 Effects of $PM_{2.5}$

$PM_{2.5}$ pollution cause negative effects in both human health and surrounding environment, including climate and atmospheric visibility. $PM_{2.5}$ pollution leads to a serious human health issue especially in the respiratory system. The small size of particulate matters can get deep into the lung and blood system. Respiratory disease such as asthma, chronic bronchitis, and lung cancer are caused by particulate matters. PM can affect both long-term and short-term impacts on human health and they can be found in the environment for a long time. Therefore, PM can enter the blood vessel through the respiratory system and these lead to cause heart rate irritation, plasma viscosity, and blood pressure changes. (Figure 2.4) Short-term exposure to $PM_{2.5}$ can result in an increase in morbidity in vulnerable groups such as children, the elderly, and pregnant women due to cardiovascular and respiratory diseases induced by particle inhalation. Some $PM_{2.5}$ particles may include hazardous components that have been adsorbed onto their surfaces. While pollens and fungi with a diameter greater than PM10 cannot penetrate the lung as deeply as tiny particles, they can cause injury to the upper respiratory tract.

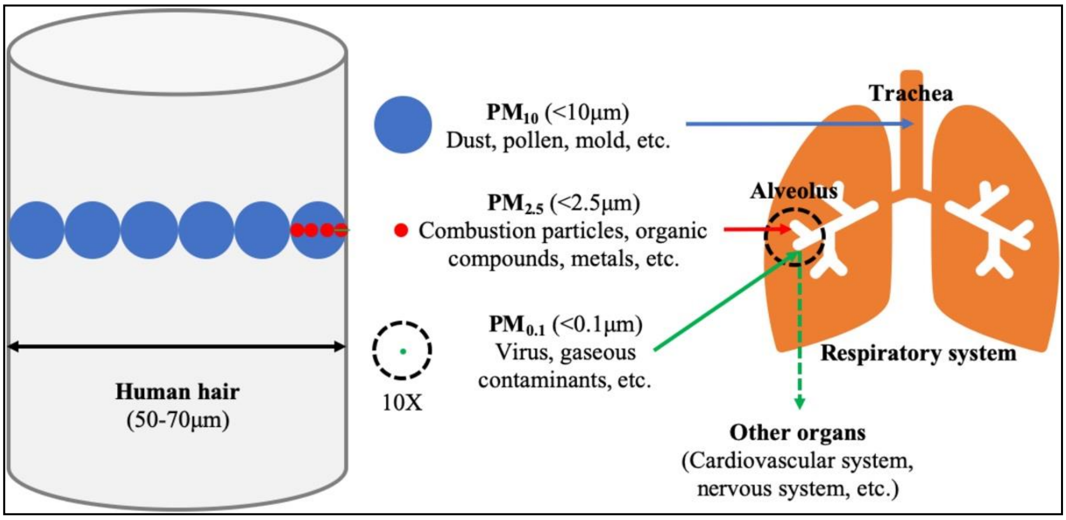

Figure 2.5: Deposition of PM in human lung

PM can influence the global and local climate in two different ways which are direct effect and indirect effects. By scattering and absorbing radiation, PM have a direct effect on the Earth's radiative balance. They have an indirect impact on the climate by changing the characteristics and conditions of clouds. Aerosols' principal direct effect is to brighten the earth when viewed from space, as the majority of aerosols scatter more than 90% of the visible light that reaches them. Aerosols have three main indirect impacts on clouds: a rise in cloud brightness, a change in precipitation, and an increase in cloud lifespan. Additionally, particulate pollution has an effect on visibility. Reduced visibility is the most visible symptom of air pollution. It is caused by the absorption and scattering of light in the atmosphere by particulate matter and gases prior to it reaching the observer. When PM concentrations rise, light is absorbed and scattered at a greater rate, resulting in decreased clarity and visual range. The most effective particles for lowering visibility are those with a diameter of 0.1-1.0m. Additionally, $PM_{2.5}$ pollution has a number of harmful consequences on the environment, including acid deposition, material and structural damage, and increased ozone levels.

2.3 Aerosol Optical Depth (AOD)

The atmospheric aerosol participates in various physical and chemical processes in the atmosphere and they are responsible for changing the chemical composition of the atmosphere and affect various environmental and human health effects. (Kouimtzis & Samara, 1995) Aerosols are tiny particles that suspended in the atmosphere or other environment. They can be emitted by human activities and natural events. Natural events such as volcanoes eruptions, windblown dust from dry and semi-arid regions, biomass burning generate aerosols into the atmosphere. Anthropogenic aerosols are generated from industrial combustion, vehicle emissions, and agricultural crop burning and commercial uses. Aerosols have different life time ranging from a few days to week and they can travel over long distances depending on the seasonal conditions. Their shapes are irregular form and sizes vary from nanometers to micrometers. Aerosols are the most important geophysical parameters in the atmosphere and they control the earth’s energy balance and hydrological cycle. These particles scatter solar radiation back, absorb solar radiation in the atmosphere, and shade the earth’s surface. Aerosols can affect the physical and environmental impacts such as human health problems and reducing visibility**.** Aerosol Optical Depth (AOD) is the most important parameter for the remote assessment of the aerosol load in the atmosphere. It is quantitative estimate of the number of aerosols in the atmosphere which are distributed within a column of air from the earth’s surface to the top of the atmosphere. AOD is also known as Aerosol Optical Thickness (AOT). Satellite remote sensing and ground-based observations have been widely used to monitor the spatial and temporal distributions of aerosols on a global and local scale. (Filonchyk et al., 2019)

2.3.1 Moderate Resolution Imaging Spectroradiometer (MODIS)

Aerosol Optical Depth is produced as standard products from Moderate Resolution Imaging Spectroradiometer (MODIS) deep blue algorithm and dark target algorithm. MODIS sensors have been attached aboard the National Aeronautics and Space Administration (NASA)'s Earth Observing System (EOS) satellite platforms, Terra since December 1999 and Aqua since May 2002. These satellites are sun-synchronize orbits with the heigh of 705 km from the earth surface. Terra passes from north to south across the equator in the morning, while Aqua passes south to north over the equator in the afternoon. MODIS has 36 wavelength channels ranging from 0.41 t0 14µm at moderate spatial resolutions (250m, 500m and 1 km) and temporal resolution of 1 to 2 days (Bilal et al., 2013). Data products derived from MODIS play an important role to develop and validate global Earth system models in order to apply in addressing global environmental issues. MODIS sensors use bands 1-7 to detect land, cloud and aerosol with different bandwidth.

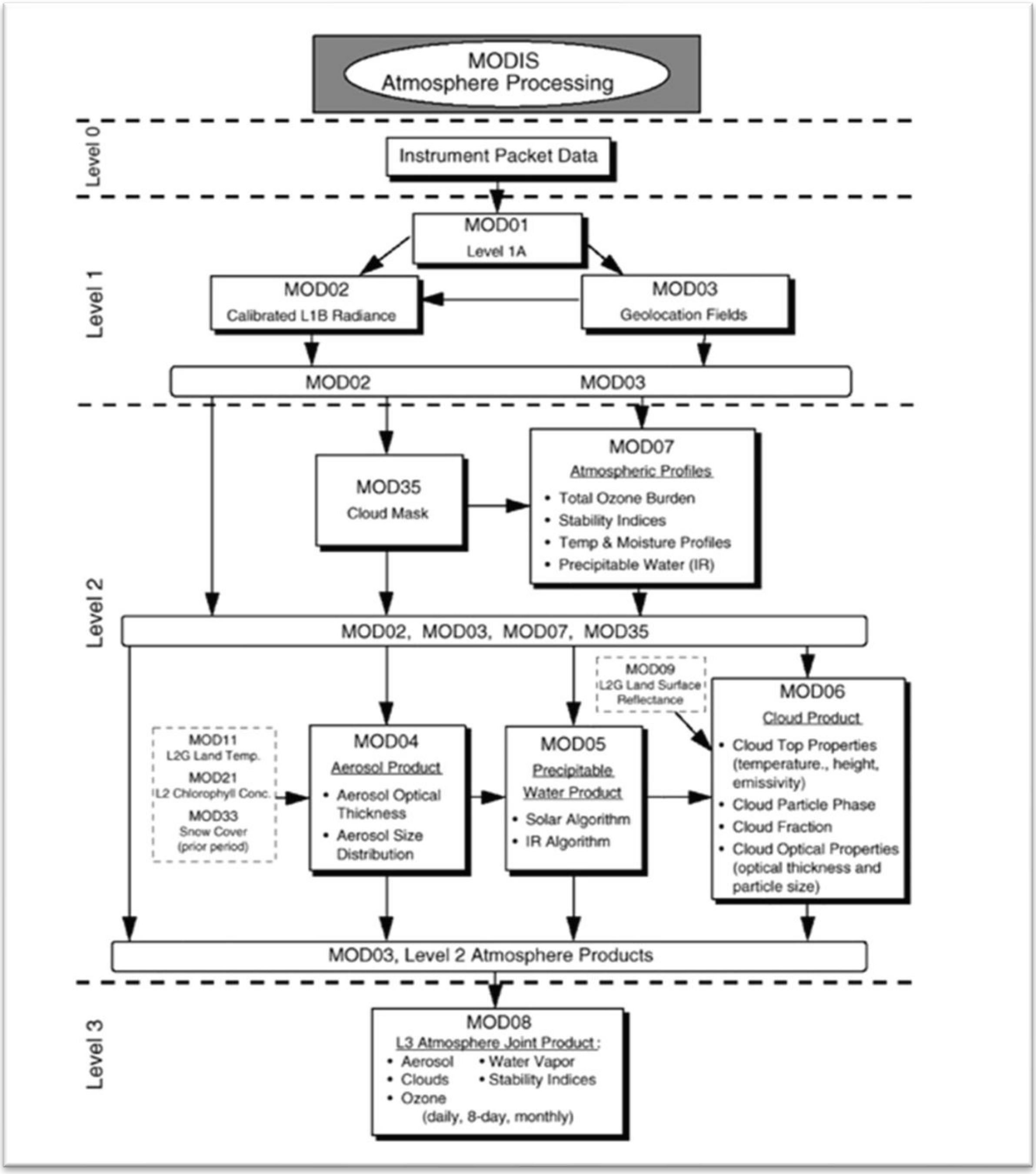

Figure 2.6: Atmospheric product provided by MODIS sensor (NASA)

Multi-Angle Atmospheric Correction (MAIAC) is a new algorithm for obtaining AOD from the Terra and Aqua sensors of MODIS. MAIAC can achieve a spatial resolution of 1 km and a high degree of accuracy in terms of AOD. The MAIAC algorithm utilizes time series analysis to determine the spectral surface reflectance required for aerosol retrieval. The combination of time series and geographical analysis contributes to the improvement of cloud and snow detection quality. MAIAC AOD retrievals have been used to predict $PM_{2.5}$ distributions and to help epidemiological studies on air pollution. (Xiao et al., 2017) MAIAC provides daily Surface Reflectance at 1 km (MCD19A1), Aerosol characteristics (MCD19A2), and an 8-day Spectral BRDF/albedo product (MCD19A3). These product files are stored in the Hierarchical Data Format (HDF), a multi-object file format designed for the exchange of scientific data in a dispersed multi-platform environment. The MCD19A2 AOD data product provides Science Dataset (SDS) layers, which are indicated in Table (2.1).

Table 2.1: Specification of Different Layers from MAIAC

SDS Name	Description	Unit	Data Type
Optical_Depth_047	Green band (0.47μm) aerosol Optical depth over land	N/A	16-bit signed integer
Optical_Depth_055	Green band (0.55μm) aerosol Optical depth over land	N/A	16-bit signed integer
AOD_Uncertainty	AOD Uncertainty based on blur-band surface brightness (reflectance)	N/A	16-bit signed integer
FineModeFraction	Fine Mode Fraction for ocean	N/A	16-bit signed integer
Column_WV	Column water vapor (cm) over land	cm	16-bit signed integer
Injection_Height	Smoke Injection height (m above ground)	meters	32-bit floating point
AOD_QA	AOD QA	N/A	16-bit unsigned integer
AOD_MODEL	AOD model used in retrieval	N/A	8-bit signed integer
cosSZA	Cosine of Solar zenith angle (5km)	N/A	16-bit signed integer
cosVZA	Cosine of View zenith angle (5km)	N/A	16-bit signed integer
RelAZ	Relative azimuth angle (5 km)	N/A	16-bit signed integer
Scattering_Angle	Scattering Angle (5 km)	N/A	16-bit signed integer
Glint_Angle	Glint Angle (5 km)	N/A	16-bit signed integer

(Source: NASA Earth Data, 2018)

2.3.2 Hamawari-8 Satellite

Hamawari-8 is a Japan Meteorological Agency-operated geostationary weather satellite (JMA) and was successfully launched by JMA in October 2014 and began operations in July 2015. Himawari-8 provides meteorological information and services in a variety of sectors, including weather forecasting, climate monitoring, and natural disaster mitigation. Himawari-8 is equipped with the Advanced Himawari Imager (AHI), which features 16 observation bands, including three visible bands, three near-infrared bands, and ten infrared bands. Himawari-8 provides a time period of ten minutes between full-disk observations. Additionally, it offers highly accurate distributions of volcanic ash and aerosols. The data from Himawari-8 is used for cloud photography, weather prediction, and a few other related sectors, where it is used to calculate quantities such as temperature and wind speed/direction in the atmosphere. Aerosol Optical Depth (AOD) products generated from Himawari-8 have a spatial resolution of 5 km and a temporal resolution of 10 minutes. Table 2.2 shows many forms of AOD that can be produced from Himawari-8.

Table 2.2 Himawari-8 Aerosol Optical Depth (AOD) Products

Type of AOD	Variables	Description
L2AOD	• AOD	• Aerosol Optical Depth at 500 nm
	• AOD_uncertainty	• Uncertainty of AOD
	• AE	• Angstrom exponent
	• QA_flag	• Quality flag
L3 hourly AOD	• AOD_merge	• Spatiotemporal interpolation of AOD_Pure
	• AOD_pure	• L2 AOD with strict cloud screening
	• AOD_L2mean	• Average of L2 AOD for each pixel
	• AOD_L2num	• Total number of L2 AOD within an hour
	• AE_merge/AE_pure/ AE__L2mean/ AE_L2num	• Angstrom exponent of each AOD variables
	• QA_fiag_merged/ • QA_flag_pure	• Quality flag of AOD and AE merge/ Quality flag of AOD and AE pure
L3 Daily/monthly AOD	• AOD_L2mean	• Temporal Average of L2 AOD for each pixel (Daily/Monthly) • calculate from: Σ (AOD_L2mean * AOD_L2num) / Σ(AOD_L2num)
	• AOD_merge_mean	• Temporal Average of AOD_merge for each pixel (Daily/ Monthly)
	• AE__L2mean	• Temporal Average of L2 AE
	• AE_merge_mean	• Temporal Average of merge AE

(source: Jaxa Earth Observation Research Center [EORC], 2020)

2.3.3 Ground-based AOD (AREONET)

AOD is measured using a ground-based sensor that uses a sun-photometer to collect both direct and diffuse solar energy in different narrow spectral bands. The Aerosol Robotic Network (AERONET) is a ground-based remote sensing network that monitors the aerosol conditions in the atmosphere using sun photometers. AERONET had been established by NASA and Physic, Optoelectronics, and Technology of Novel Micro-resonator Structures (PHOTONS).These data allow for the determination of important optical parameters such as aerosol optical depth (AOD), Angstrom exponent (AE), single scattering albedo (SSA), and size distribution. (Janjai et al., 2012) AERONET provides information on the spectrum aerosol optical depth (AOD), inversion products, and precipitable water in a wide variety of aerosol regimes. Aerosol optical depth data are generated at three different levels, 1.0, 1.5, and 2.0 of data quality which have (unscreened), (cloud-screened), and (cloud screened and quality-assured), respectively. AERONET is a global network of around 140 stations. All stations collect and measure solar radiation at a variety of nominal wavelengths, including 340, 380, 440, 500, 675, 870, 1020, and 1640 nm. (Janjai et al., 2012) The figure (2.6) illustrates the AODs data from AERONET's Chiang Mai station during 2020.

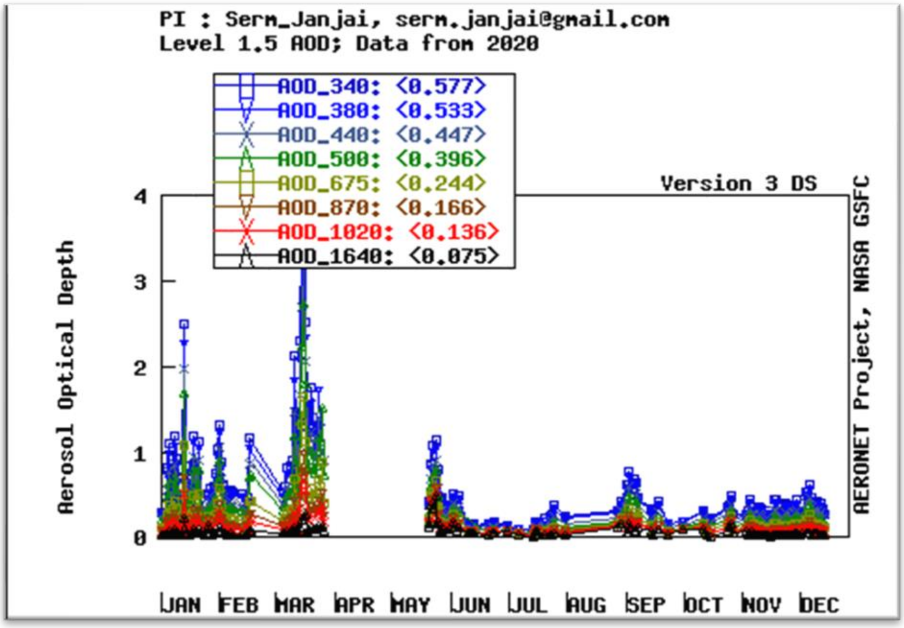

Figure 2.7: AOD information from AERONET in Chiang Mai Station (NASA, 2020)

2.4 Remote Sensing

Method of remote sensing is a data collecting process for information about the earth without taking an actual sample from the surface of the earth. This process uses sensors to collect data from a distance. Sensors measure and analyze the reflected energy from the atmosphere and earth surface. These information are displayed as digital images or photographs. Sensors are attached on a satellite, a plane or other air vehicles. Remote sensing base on the different electromagnetic Radiation and collects the data by many different wavelength bands. The sun radiates energy for Remote sensing. This energy is either reflected or absorbed and then re-emitted by the objects on the earth and in the atmospheric condition.

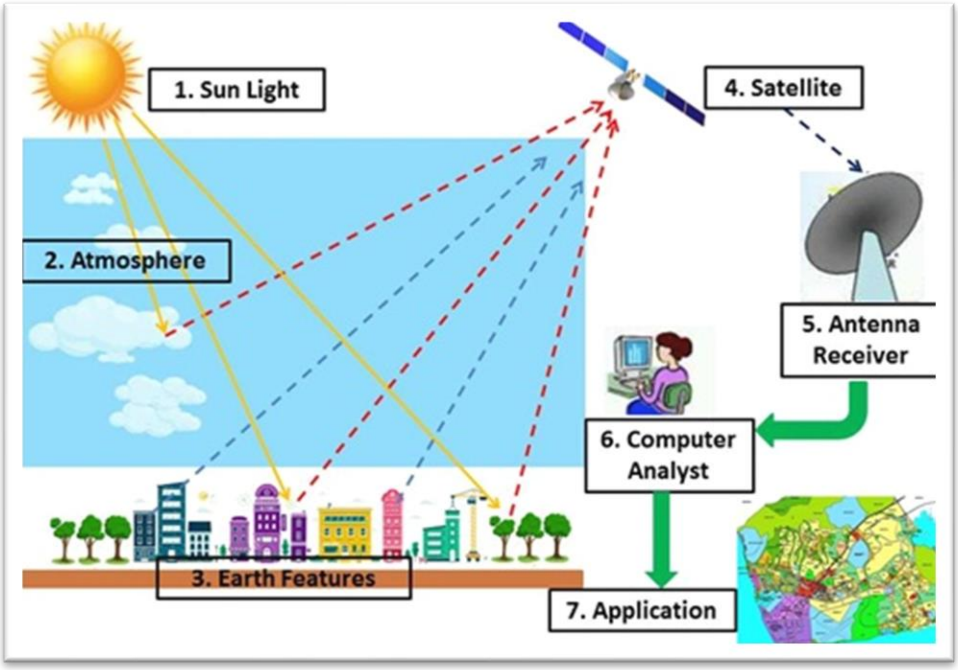

Figure 2.8: Processes of remote sensing

Sensors are divided into two types known as Active and Passive Sensor. Active sensors use the energy that is emitted by itself to collect the reflection of the target objects. Active sensors have the ability to obtain the information anytime, regardless of the time of day and season. Passive sensors can only be used to detect natural energy that come from the sun. Therefore, passive sensor can detect the radiation during only day time, and they cannot be used in cloudy condition.

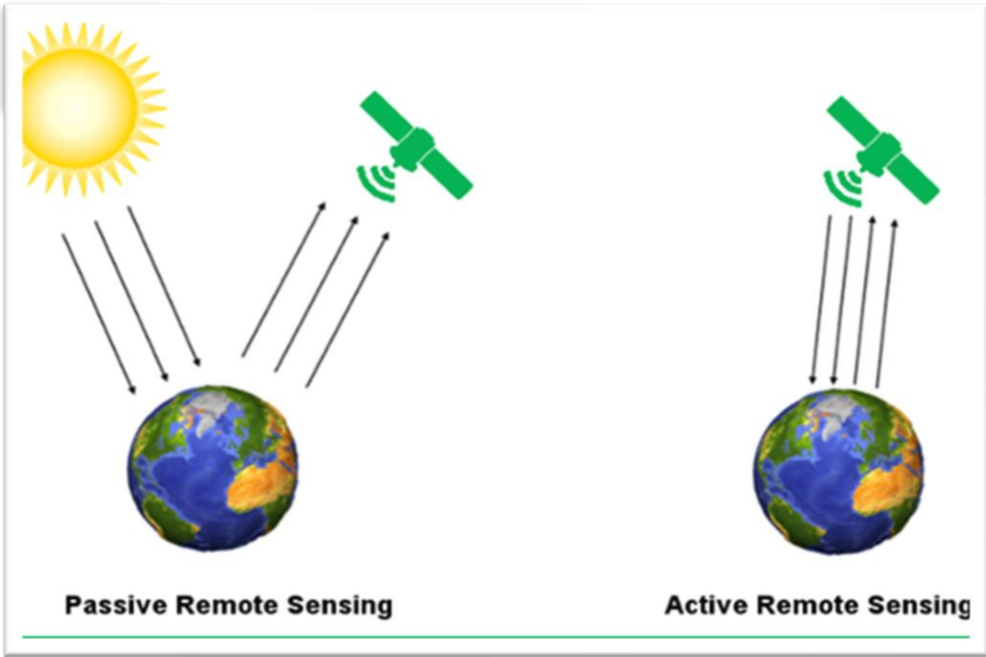

Figure 2.9: Passive and Active sensor in Remote sensing

Remote sensing applications are widely used in environmental assessment, mapping of land use and land cover, weather forecasting, and earth analyzing field. However, the information from remote sensing needs to be evaluate or validate with the actual information called ground-based data to get the high accuracy.

2.5 Satellite Image

Satellite images are any image of the earth that are taken from the satellites. These images are very effective for remote sensing of the earth's information of the target area. The system of satellite image procures and classifies electromagnetic energy reflected from the earth surface and atmosphere. There are many different wavelengths in the electromagnetic spectrum such as microwave, visible light, infrared, and ultraviolet. Sun is the major source of EM energy. The satellite image identifies the types of object such as water, forest, building by the different strength of the reflection or radiation. The quality of satellite images depends on the type of energy sources, sensor resolutions, atmospheric interference, real-time energy reflectance or absorption values, and data handling systems.(Borra et al., 2019)

2.5.1 Temporal and Spatial Resolution

Resolution of a satellite image is a parameter which defines the ability to detect, recognize, and distinguish between various objects and their qualities. There are four types of satellite image resolution known as spatial, spectral, temporal, and radiometric resolutions. Spectral resolution is proportional to the width, sensitivity, position, and number of spectral bands. The radiometric resolution of a scanner/sensor is the number of gray levels utilized to represent the data in an image form. It is determined by the bit depth utilized to show each pixel value. The high radiometric resolution enables the observation of minute variations in reflectance. Spatial resolution is the size of one pixel on the surface of earth. If the spatial resolution is 5 kilometers, it means that one pixel on the image is equal to a square of 5 kilometer by 5 kilometers on the ground. Sensor with high spatial resolution cover the smaller area than the one with the same number of pixels and with lower spatial resolution. Temporal resolution is the measurement of time needed to acquire data for the exact same location. In remote sensing, this resolution depends on the sensor and orbital characteristics of the sensor platform. The higher temporal resolution means the shorter the period of time. Temporal resolution can vary from hours to days. Most satellites have a medial temporal resolution of about 14 days but there are some satellites which have 15 minutes resolution. This high temporal resolution satellite sensors are used as weather satellites but they usually have low spatial resolution.

2.6 Air Quality Standards in Thailand

Ambient air quality standards are one of the most important tools to implement effective air quality management system. These standards need to be set up based on the consideration of public health, technologies, policies, and economy status. Ambient air quality standards are commonly issued for the major air pollutants such as Particulate Matters ($PM_{2.5}$, PM_{10}), Sulfur dioxide, Carbon dioxide, Nitrogen dioxide, Ozone, heavy metal and so on. Thailand's 1992 Enhancement and Conservation of the National Environment Quality Act established National Ambient Air Quality Standards (NAAQs). Table (2.3) shows the values of air pollutant concentration in Thailand's national ambient air quality standards (NAAQs).

Table 2.3: Standard Values of Air Pollutants in NAAQs Thailand

Pollutants	Unit	Standard Values				
		1-hr avg	8-hr avg	24-hr avg	1-month avg	1-year avg
CO	ppm	30	9	-	-	-
NO_2	ppm	0.17	-	-	-	0.03
SO_2	ppm	0.3	-	0.12	-	0.04
O_3	ppm	0.1	0.07	-	-	-
TPS	mg/m^3	-		0.33	-	0.1
PM_{10}	mg/m^3	-		0.12	-	0.05
$PM_{2.5}$	mg/m^3	-		0.05	-	0.025
Lead (Pb)	mg/m^3	-	-	-	0.0015	-

2.6.1 Air Quality Index (AQI)

Air Quality Index (AQI) is an index which is used for reporting air quality on a daily basis. AQI shows the effects human's health within a short time period due to air pollution. The main objective of AQI is to provide people know how the local air quality impacts their health. In Thailand, the Air Quality Index (AQI) is separated into five different levels based on the concentration of six different air pollutants. These pollutants are particulates (PM_{10} and $PM_{2.5}$), sulfur dioxide (SO_2), carbon monoxide (CO), ozone (O_3), and nitrogen oxide (NO_x) Table (2.4) shows the AQI levels and how they can hurt your health (2.4).

Table 2.4: Air Quality Index (AQI) Level of Thailand

AQI	Level	Color	Description
0-25	Excellent	Blue	The air quality is determined to be acceptable, and it is suitable for outdoor activity.
26-50	Satisfactory	Green	The air quality is assessed to be good, and the public can participate in outdoor activities.
51-100	Moderate	Yellow	Sensitive group: Reduce continuous or heavy exhaustion and keep an eye on symptoms (e.g., coughing or shortness of breath).

AQI	Level	Color	Description
			General Public: It is unlikely to be harmed, and the general public will have access to outdoor activities.
101-200	Unhealthy	Orange	Sensitive people: You might want to use personal protection equipment. Avoid doing too much for a long time. Call your doctor if anyone in the public is having problems (like coughing or shortness of breath, eye irritation, or something else). General public: If you do a lot of long or heavy work, you might want to cut back on it and watch for symptoms (e.g., coughing or shortness of breath). Consider wearing personal safety equipment.
>201	Very Unhealthy	Red	Everyone should not do any physical outdoor activities or stay away from places with a lot of air pollution.

(source: PCD, 2019)

2.7 Meteorological Data

Meteorology is the study of the atmosphere to understand the physical, dynamic, and chemical state and the interaction with the surface of the earth. Meteorological data are a collection of information on the atmosphere's features. The data for a single day or a specific time period during the day is referred to as the weather condition, while the data for a longer period is referred to as the climate of the place. Some important meteorological parameters are temperature, precipitation, humidity, solar radiation, and wind speed and direction. These parameters are very important in environmental air pollution. Emission,transportation, dispersion, and deposition of air pollutants are directly or indirectly controlled by these parameters. In the monitoring and management of air pollution, meteorological data are the major information to get the high accuracy of the result.

Wind speed and direction are the most important factors in monitoring and predicting of air pollution, weather conditions and global climate. They can affect many impacts on the distribution of air pollutants and aerosol emissions. Wind speed is measured as the unit of miles per hour, knots, or meter per second. The wind direction is expressed in degrees and indicates the direction in which the wind is blowing. A direction of zero degrees indicates a northerly wind. Wind speed is determined using a cup or anemometer, a device consisting of three cups of propellers mounted vertically. The wind force spins the cups, and the rate at which they spin is related to the wind speed. Some monitoring station use the sonic anemometer which conduct base on the wavelength and this can measure both wind speed and direction. Wind direction is indicated by a wind vane that aligns with the wind direction.

Wind direction is different in the northern and southern hemisphere by Coriolis force. Wind rose is used to illustrate the condition of wind speed and direction on the circle bar scale and percentage of the wind speed. Wind speed is proportional to the height from the earth's surface. Wind speed depends on the fraction of the surface. In urban area with high building, the wind speed is lower than in rural area.

Atmospheric temperature is one of the meteorological parameters that affect the conditions of air pollutant. Sunlight is the source of atmospheric temperature and it takes place some chemical reactions in the atmosphere. Air temperature has inverse proportion with elevation. Air near the ground is warmer than air far from the earth's surface. During cold weather, emission from vehicles, industries and crop burning is more visible. PM concentrations usually increase during this situation.

Humidity is also a significant factor which determines the movement of air pollutant in troposphere due to the distribution of electrical charges on particles. Humidity is the amount of water vapor expressed as a percentage of maximum amount of water vapor in the air at a given temperature.

2.8 Resampling

An image resampling is a process that occurs when the raster structure of the image changes, for example, by changing the projection, reprojecting the image, changing the datum, or changing the size of the cells (Wade & Sommer, 2006). There are many different methods to scale down raster images, depending on whether the image is enlarged or reduced, in which the raster boundaries stay the same and only the structure of the image changes. Most popularly used resampling methods are nearest neighbor, bilinear and bicubic.

The nearest neighbor resampling is one in which a pixel from the original image is matched to its corresponding place in the scaled image. If the relevant pixel value is not accessible, the value of the closest pixel is utilized instead. The primary advantage of nearest neighbor resampling is that it keeps original values and does not generate interpolated values, making it the closest approximation of the picture. Additionally, due to its ease of implementation and simplicity, it is the most extensively used method for picture resampling. A significant downside of this approach is that it creates position inaccuracies in areas where pixel realignment is visible, particularly along linear structures. This resampling technique is optimal for displaying categorical data, such as nominal and ordinal values.

The bilinear resampling method generates a new pixel value by taking the arithmetic mean of the target cell's adjacent four pixels. Because it is an interpolated value, it is possible for a new value to be introduced that was not present in the original raster picture. Bilinear resampling methods produce a smoother appearance and maintain a higher level of positional accuracy than closest neighbor resampling methods, making them particularly helpful for continuous data without identifiable borders. However, averaging might introduce local peaks and valleys, increasing error propagation when compared to the nearest neighbor.

Cubic resampling is a resampling technique which uses a weighted average of the sixteen (16) pixels adjacent to the target cell. Bicubic resampling is a variation on the cubic resampling technique in that it does resampling in both the X and Y dimensions. This approach is suitable for continuous data with a high level of noise. Resampling creates a smoother surface than nearest neighbor or bilinear resampling, but it is more costly than the other resampling methods due to the increased number of surrounding cells.

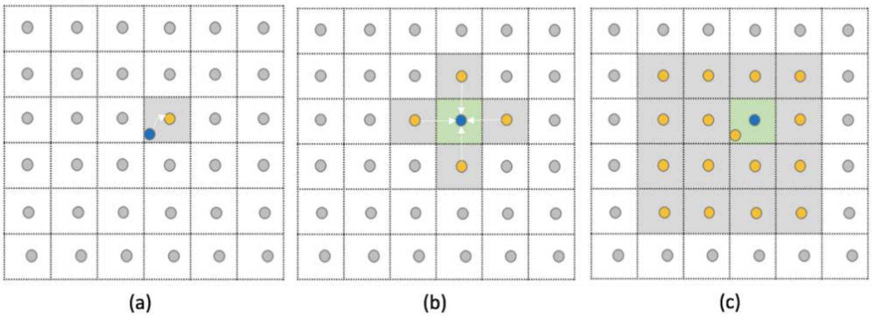

Figure 2.10: Different Types of resampling (a) Nearest neighbor (b) Bilinear (c) Cubic

2.9 Random Forest Regression

Random Forest is a supervised machine learning technique that is built on the foundation of decision tree algorithms. This technique is used to address regression and classification problems, and it solves them by combining many classifiers. Random Forest Regression (RFR) generates the output from the decision trees' predictions. It averages the output from many trees. A random forest algorithm's building pieces are decision trees, which have a tree-like structure. The principle of Random Forest Regression is identical to that of simple regression. The random forest model passes the values of dependent and independent variables. Each tree in RFR generates a unique forecast. The regression result is the mean forecast of the individual trees. RFR is used in a variety of industries, including banking, health care, the stock market, and e-commerce.

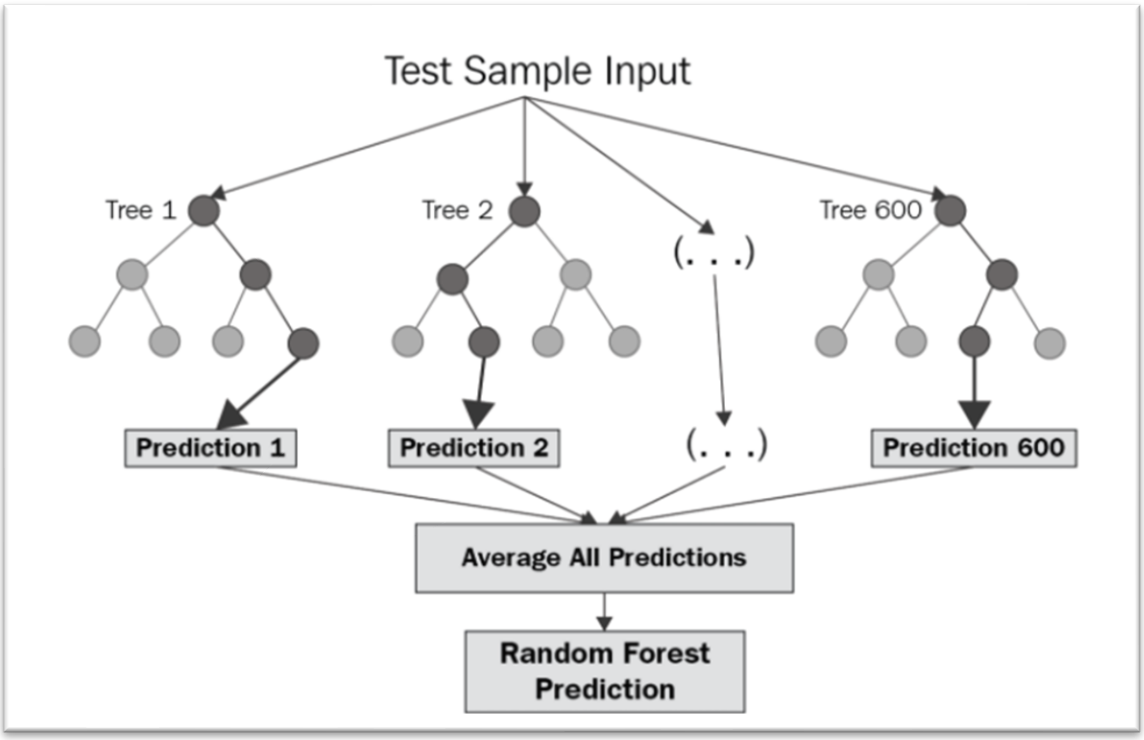

Figure 2.11: structure of Random forest Regression

2.10 Current Research

Samermit (2020) used hourly aerosol optical depth data from the Himawair-8 satellite to estimate the $PM_{2.5}$ concentration in Chiang Mai Province. This study concentrated on the months of February and April (2017-2019). The link between ground-based $PM_{2.5}$ concentration and AOD products produced from Himawari-8 was determined using hourly 5 km spatial resolution AOD products. For the research period, ground-based AERONET's Aerosol Optical Depth (AOD) data were obtained at the Chiang Mai station. Correlation analysis was performed in two ways in this study: with and without meteorological data. The Himawari-8 satellite's AOD L2mean variables were used to indicate the average aerosol loading from 09.00 to 16.00 LT in February through April (2017–2019) and were compared to ground-based AOD from AERONET. The validation of Himawari-8 AOD and AERONET AOD in the Chiang Mai revealed a high degree of agreement, with a correlation coefficient of R^2 0.57 and a RMSE of 0.38. As a result, the AERONET AOD underestimated 55.4 percent of the Himawari-8 AOD. The link between Himawari-8 AOD and $PM_{2.5}$ concentrations measured at a ground-based monitoring station in Chiang Mai was determined using linear regression. The R2 values for the hourly AOD and $PM_{2.5}$ relationships without and with meteorological parameters are 0.39 and 0.75, respectively. The link between AOD and $PM_{2.5}$ with meteorological parameters demonstrated the best model performance, with a correlation coefficient of 0.75 and the standard error of estimation (30.9).

According to Jansakoo (2020), the Bangkok Metropolitan Region's $PM_{2.5}$ concentration was estimated using high resolution AOD collected from satellites in combination with land use and meteorological data. This study used AOD outputs with a spatial resolution of 500 x 500 m^2 from the MODIS sensor on the Terra and Aqua satellites. The high spatial resolution of AOD with $0.5km^2$ based on the MODIS sensors was developed using the Simplified high-resolution MODIS Aerosol Retrieval Algorithm (SARA). The SARA-AOD and MODIS standard products were validated against ground-based AERONETs' AOD data, and the results indicated that the relationship between SARA-AOD and AERONETs' AOD was stronger than the relationship between the MODIS AOD and AERONETs' AOD (R2 0.73 vs. R2 0.62). The link between the SARA-AOD and the ground-based $PM_{2.5}$ concentration, on the other hand, was weak, with an R2 of 0.123. Meteorological and land-use data were used as additional inputs to develop empirical models for estimating $PM_{2.5}$ concentrations using multi-linear regression (MLR), artificial neuron network (ANN), and land-use regression (LUR). The MLR model performed the best on an independent dataset (R^2 = 0.420), followed by the LUR model (R^2 = 0.291) and the ANN model (R^2 = 0.125).

2.11 Research Gaps

According to the previous studies on $PM_{2.5}$ estimations using satellites derived Aerosol Optical Depth, the AOD with high spatial resolution of 500 x 500 m^2 from SARA-MODIS has very low temporal resolution (2 times per day) due to the orbit of the satellites. Spatial resolution of AOD products from Himawari-8 is very low with 5 x 5 km^2, but it has high temporal resolution of every 10 minutes. Chiang Mai has the limitation of ground-based air monitoring stations to provide $PM_{2.5}$ concentration over the whole area. The estimation of $PM_{2.5}$ concentration with remote sensing will be necessary for the whole area of Chiang Mai. High resolution AOD with 1x1 km^2 spatial resolution and hourly temporal resolution from the combination of two different AOD products which are derived from MODIS-MAIAC and Himawari-8 was developed, and used for $PM_{2.5}$ concentration prediction.

Chapter 3

Methodology

This study used Aerosol Optical Depth with an hourly spatial resolution of 1 x 1 km^2 collected from two satellites to predict the hourly $PM_{2.5}$ concentration in Chiang Mai for the year 2020. The AOD was derived from two distinct satellites, MODIS-MAIAC and Hamawari-8. There were three major steps in this research: data input collection, data processing, and output map development, as illustrated in Figure 3.1. The first step involved selecting the research region and time period, extracting AOD products, collecting ground-based $PM_{2.5}$ and meteorological data, and preparing the data. The second phase was data processing, which involved combining AOD products from two satellites, establishing a link between AOD and $PM_{2.5}$ using meteorological data, and estimating $PM_{2.5}$ concentration in Chiang Mai. The final stage is the Output phase, during which hourly 1 x 1 km^2 $PM_{2.5}$ concentration maps were created for the study area.

3.1 Framework of Methodology

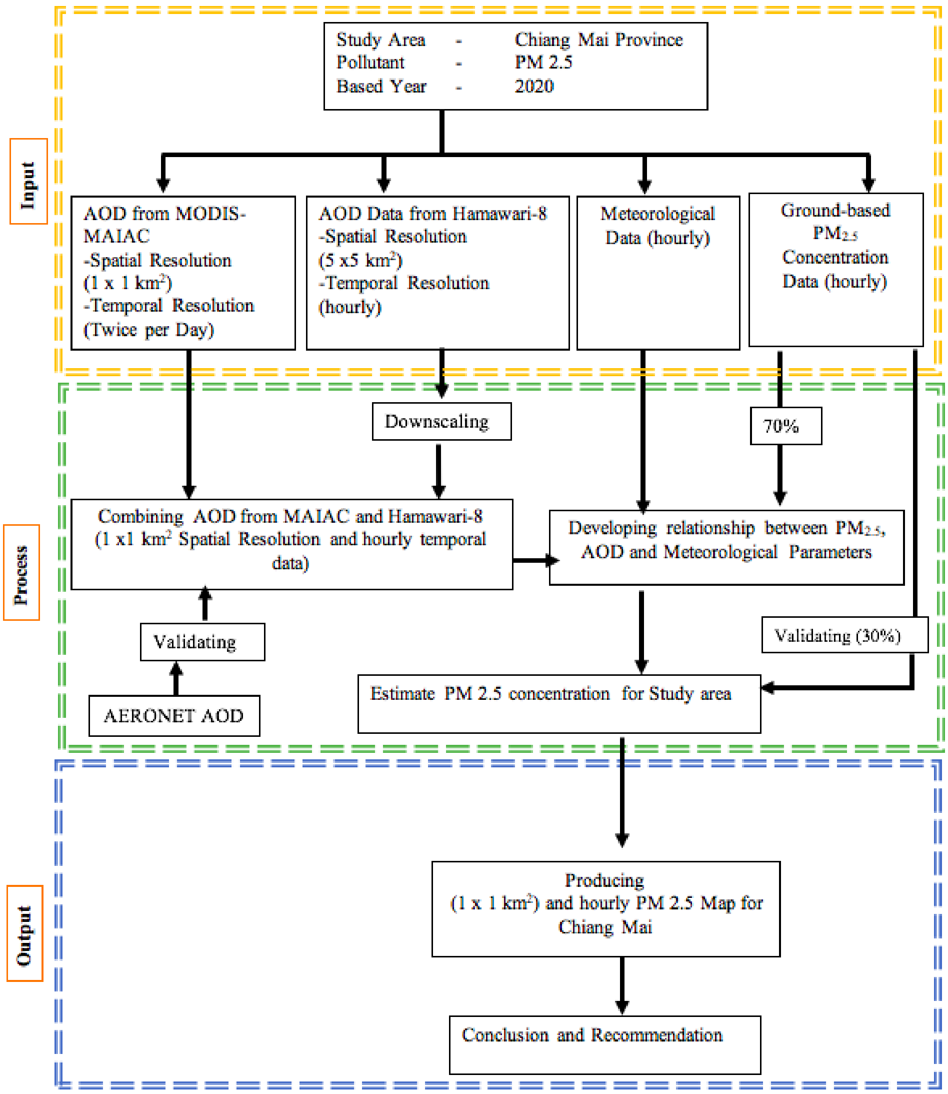

Figure 3.1: Framework of methodology.

3.2 Study Area

Chiang Mai province (Figure 3.2) was chosen as the research location; it is located at Latitude 18.7883° N and Longitude 98.9853° E and has a population around 1.7 million people at a density of 79 people/km^2 (National Statistical Office, 2019). It is divided into 25 districts and encircled by mountains and valleys. Chiang Mai has a colder temperature than the central plains near Bangkok due to its northern latitude and elevation. April and January are the hottest and coldest months, with average maximum temperatures of 36°C and 28°C, respectively. Precipitation is more in May, June, July, and October than in other months. Chiang Mai's yearly average relative humidity is 75.8 percent. This area is often faced with a problem with $PM_{2.5}$ concentrations during the dry season of each year as a result of open burning of agricultural residues and forest fires (IQAir, 2020). The study was undertaken between January and December 2020.

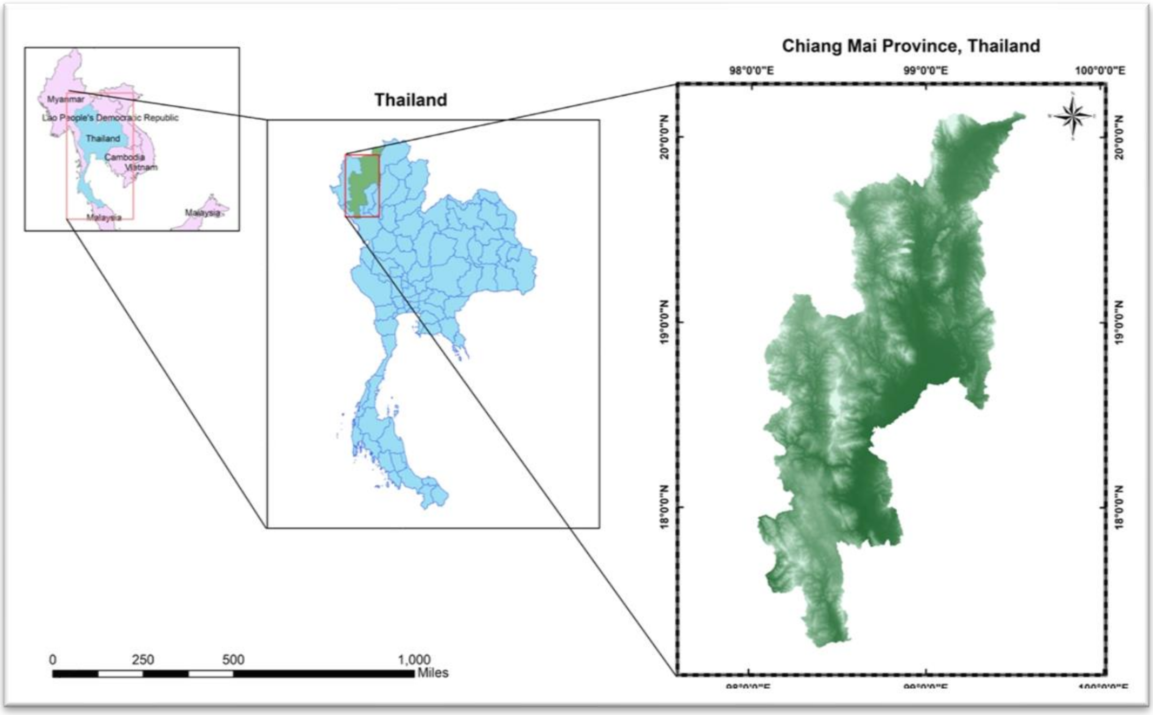

Figure 3.2: Location of the Study Area, Chiang Mai Province

3.3 Input Data

3.3.1 Satellite AOD Data

The aerosol optical depth (AOD) products from two separate satellites were used in this study: the MODIS sensor and Hamawari-8. The MODIS sensor generates AOD products with a spatial resolution of 1 x 1 km^2 using the Multi-angle Implementation of Atmospheric Correction (MAIAC), whereas the Hamawari-8 sensor generates hourly AOD products with a spatial resolution of 5 x 5 km^2. Terra and Aqua satellites are equipped with MODIS sensors and give AOD data twice daily. Daily, the satellites pass over the study area, Chiang Mai, between 10:00-11:00 a.m. (Terra) and 13:00-14:00 a.m. (Aqua), providing MAIACs' MCD19A2 Version 6 Data at a resolution of 1kilometer pixel. The MCD19A2 AOD data product includes blue band AOD at 0.47 m and green band AOD at 0.55 m, as well as AOD uncertainty, fine mode fraction over water, column water vapor over land and clouds, smoke injection height, AOD quality assurance, AOD model at 1 km, cosine of solar zenith angle, cosine of view zenith angle, relative azimuth angle, scattering angle, and glint angle at 5 km. Various AOD products from MODIS-MAIAC terra and aqua MCD19A2 can be obtained via the NASA Earth Data LAADS web (https://ladsweb.modaps.eosdis.nasa.gov/).

The Himawari-8 AOD products have a spatial resolution of 5 km and a high temporal resolution of hourly data from 9:00 to 16:00. Due to its great temporal resolution, these AOD products benefit from cloud contamination reduction. The Himawari-8 AOD products are accessible at http://www.eorc.jaxa.jp/ptree/index.html, and for hourly AOD data, the product Level-3 Version 3.0 with a spatial resolution of 5 km was used.

3.3.2 AERONET AOD Data

The National Aeronautics and Space Administration (NASA) built the Aerosol Robotic Network (AERONET), which is a network of solar photometers from aerosol ground-based monitoring systems (NASA, 2020). The performance of AOD products from two different satellites was evaluated using AERONET AOD data. From this Network, The AOD Level 2.0 Version 2 (at 500 nm) was used in this study, which includes cloud screening and quality assurance. These data were gathered at Chiang Mai Station (18.78N, 98.98E) in Thailand's northern region. This AERONET data was collected from the NASA AERONET website, which can be found at https://aeronet.gsfc.nasa.gov, for the research period of January to December 2020.

3.3.3 Ground-based $PM_{2.5}$ Concentration Data

Ground-based $PM_{2.5}$ concentration data were collected from two ambient air quality monitoring stations of the Thailand Pollution Control Department (PCD). In Chiang Mai, there are only two air quality monitoring stations which are Chiang Mai City Hall (station code 35T) and Yuparaj Wittayalai School (station code 36T). The hourly average $PM_{2.5}$ concentration data in 2020 were applied for the estimation of $PM_{2.5}$ concentration with the AOD products from the satellites. In this study, seventy-five percent (70%) of Ground-based $PM_{2.5}$ concentrations were used to develop the relationship with AOD and the remained twenty-five percent (30%) were used to validate the relationship. Table 3.1 show the information of two monitoring stations in Chiang Mai.

Table 3.1: PCD's Ground-based Ambient Air Quality Monitoring Station in Chiang Mai

Station ID	Name	Data	Location	Latitude	Longitude
35T	City Hall, Chiang Mai	Hourly $PM_{2.5}$ concentration	Chang Phueak, Meuang, Chiang Mai	18.84063	98.969661
36T	Yupparatch Wittayalai School	Hourly $PM_{2.5}$ concentration	Si Phum, Meuang, Chiang Mai	18.79092	98.9881062

3.3.4 Meteorological Data

Meteorological data were gathered from Chiang Mai air quality monitoring stations, and the hourly averages were calculated. Temperature, relative humidity, wind speed, and wind direction were all employed as meteorological parameters in this research. Information in Table 3.2 refers to meteorological data collected at two stations in Chiang Mai, and Figure 3.3 shows locations of the ground based $PM_{2.5}$ monitoring stations in this study.

Table 3.2: Meteorological Parameters from Air Quality Monitoring Station in Chiang Mai

Station ID	Name	Meteorological Parameters
35T	Chiang Mai City Hall	Temperature, Relative Humidity, Wind Speed, Wind Direction
36T	Yuparaj Wittayalai	Temperature, Relative Humidity, Wind Speed, Wind Direction

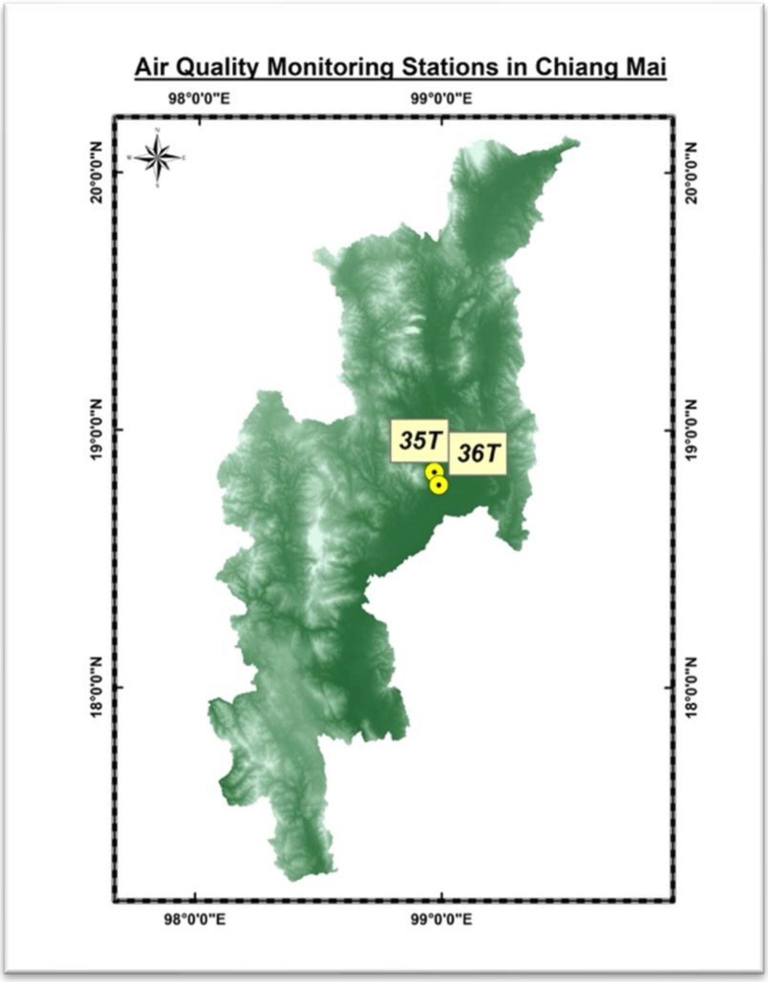

Figure 3.3: Ground-based $PM_{2.5}$ Monitoring Stations in Chiang Mai

3.4 Data Processing

3.4.1 Development of High resolution AOD

This work employed linear regression to combine AOD results from two separate satellites in order to obtain AOD products with a greater spatial and temporal resolution. MAIAC-MODIS can give data with a high spatial resolution; however, it is only available once per day. Hourly (from 9:00 a.m. to 16:00 a.m.) AOD products with a spatial resolution of 5 x 5 km^2 were collected from Hamawari-8. The resolution of Himawari-8 AOD products was downscaled from 5x5 km^2 to 1x1 km^2 using the bilinear resampling method in ArcGIS. The AOD values from MAIAC with a spatial resolution of 1 km^2 were used to find the correlation with hourly Himawari-8 AOD from 9:00 a.m. to 16:00 a.m., and hourly 1x1 km^2 resolution AOD was generated by linear regression. The flowchart of the combination between MAIAC and Himawari-8 AOD is presented in Figure 3.4. During the research period, the outcome of the integration of AOD values was checked against AOD values from AERONET.

3.4.1.1 Downscaling Himawari-8 AOD. In this process, Himawari-8 AOD with 5x5 km^2 spatial resolution was downscaled to 1x1 km^2 resolution by resampling method. The AOD values from himawari-8 satellites were extracted as raster layer from NetCDF file format by Multidimensional tools in ArcGIS. These raster layer with 5km^2 pixel size were downscaled to create 1km^2 cell size by resampling method under raster processing tools. In the resampling process, bilinear method was applied, and bilinear interpolation was used to create new value of a pixel from weighted distance average of four nearest input cell. After downscaling, AOD value which have 1km^2 resolution from MAIAC and Himawari-8 were extracted by using extract value to point tool under spatial analyst tools in ArcMap. The value extracted from each raster cell were used to determine the relationship between AOD products from these two different satellites. The linear regression was used to develop the relationship in each hour from 09:00 to 16:00 hr. with MAIAC AOD values derived from averaging Terra (10:00 hr.) and Aqua (13:00 hr.). Figure 3.4 shows the process of integration AOD from two different satellites, MAIAC and Himawari-8.

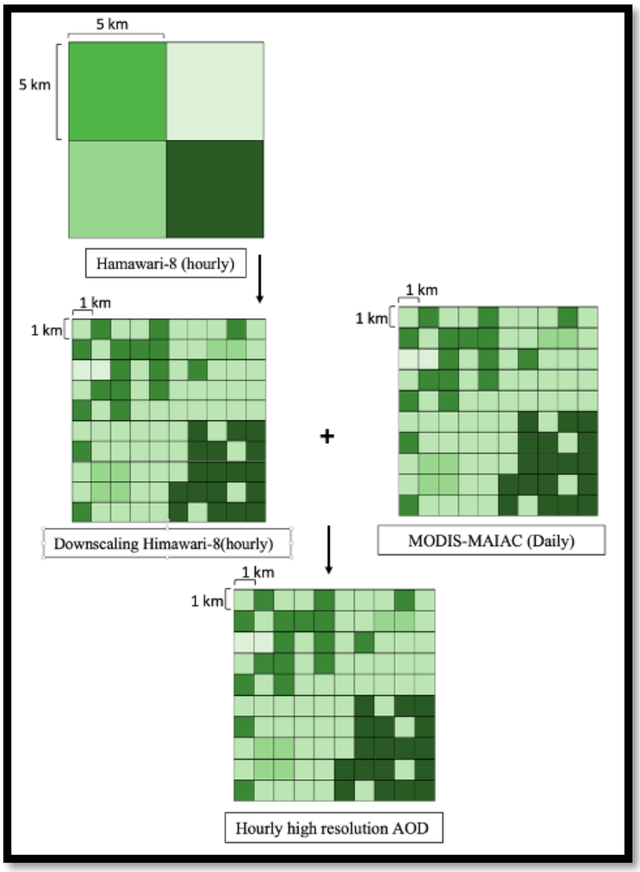

Figure 3.4: Integration of AOD with Different Resolution from two Satellites

3.4.2 Validation of AOD data

AOD data from the AREONET station in Chiang Mai were used to validate the AOD data obtained through the integration of two satellites. These AOD have different spatial and temporal resolutions with satellite derived AOD. To obtain the same time and location, spatially averaged AOD measurements inside 3x3 grid cells at the AERONET station's center were used, as well as hourly averaged AOD values during the period when the satellite passes over the research region. Correlation coefficients were obtained between this AOD data and mean absolute error (MAE) and root mean square error (RMSE) values were also produced to assess uncertainty.

3.4.3 Developing relationship AOD and Ground-based data

Hourly high spatial resolution AODs from two satellites generated from integration method and hourly ground-based $PM_{2.5}$ concentration data were applied to develop a relationship equation with meteorological data during the study period. In this process, multiple linear regression(MLR) technique was used to development an equation to estimate $PM_{2.5}$ concentration. Meteorological parameters with the same time scale as $PM_{2.5}$ data were used to get higher performance for the estimation of the $PM_{2.5}$ concentration. The Equation of Multiple Linear Regression were applied (Equation 3.2):

$$Y = a + b_1X_1 + b_2X_2 + b_3X_3 + b_4X_4 + \cdots + b_nX_n + \epsilon \quad \text{(Eq 3.1)}$$

Where, Y = Dependent variable,
X = Independent variable,
a = Y-Intercept
b = Slope coefficients for each explanatory variable, and
ϵ = model's error term

In this process, Random Forest Regression (RFR) was also applied to compare the result of the relationship between high resolution AOD and ground-based data. For RFR, scikit-learn from Python machine learning toolkit was used. Firstly, $PM_{2.5}$ data were identified as dependent variable and AOD, temperature, relative humidity, wind speed and wind direction were independent variables. These datasets were split into training and testing set. RFR model trained the dataset to predict with testing data and finally the result was showed R^2 score that tell how well model is fitted to the data.

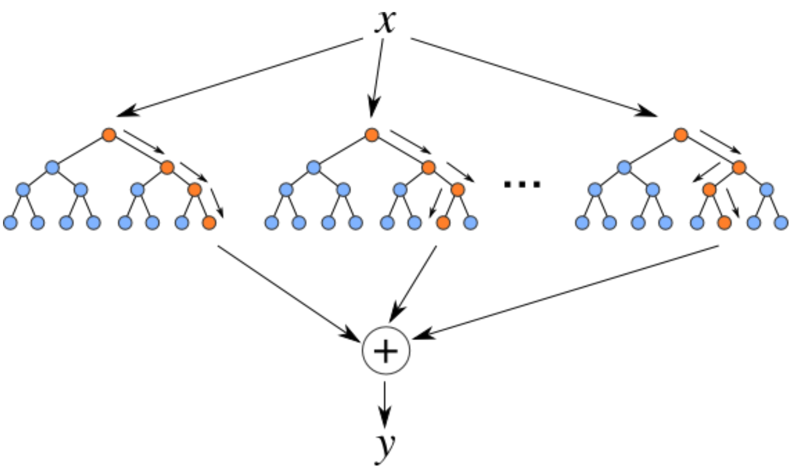

Figure 3.5: Random forest regression diagram

3.4.4 Estimation of $PM_{2.5}$ concentration

The $PM_{2.5}$ concentration in the study area for 2020 were estimated from the hourly high spatial resolution AOD from the linear regression result which provided the highest R^2. These estimated $PM_{2.5}$ concentration will be compared with the ground-based $PM_{2.5}$ concentration of 2020. The performance of $PM_{2.5}$ model was evaluated with the statistical analyses, i.e., Root Mean Square Err (RMSE) and Mean Absolute Err (MAE) as presented in Equation 3.4 - 3.5, and the criteria for evaluating of each statistical parameter is provided in Table 3.3.

$$MAE = \frac{1}{n}\sum\left|y_{observed} - y_{predicted}\right| \quad \text{(Eq.3.2)}$$

$$RMSE = \sqrt{\frac{1}{n}\sum(y_{observed} - y_{predicted})^2} \quad \text{(Eq. 3.3)}$$

Table 3.3: Statistical Methods for Checking Performance

Statistics	Equation	Criteria
Mean Absolute Error	$MAE = \frac{1}{n}\sum \lvert y_{observed} - y_{predicted} \rvert$	Low value
Root Mean Square Error	$RMSE = \sqrt{\frac{1}{n}\sum (y_{observed} - y_{predicted})^2}$	Low value

3.5 Producing (1x 1) km^2 and hourly $PM_{2.5}$ Map

In this process, the $PM_{2.5}$ concentration map of Chiang Mai were estimated by the linear regression equation generated in section 3.4. Raster Calculator from the application of ArcGIS was used to generate the values of $PM_{2.5}$ over the Chiang Mai Province. To get hourly distribution of $PM_{2.5}$ concentration, four different meteorological parameters from Chiang Mai air monitoring stations were interpolated with Inverse Distance Weighted (IDW) interpolation method to cover the whole study area. The Spatial Analysis tool in ArcGIS were applied in order to extract 1 x 1 km^2 and hourly $PM_{2.5}$ concentration map. The spatial distribution maps of $PM_{2.5}$ concentration in Chiang Mai with high resolution AOD from MODIS-MAIAC and Hamawari-8 Satellites were developed during the year of 2020.

Chapter 4

Results and Discussion

This chapter is divided into three parts. First, the results of ground-based $PM_{2.5}$ monitoring data in the study area in 2020 are presented. Second, high-resolution AOD derived using data from two satellites with varying temporal and geographical resolutions are discussed. Third, the spatial distribution map of $PM_{2.5}$ concentrations derived from the hourly 1x1 km^2 resolution development is presented.

4.1 Ground-based Data

4.1.1 $PM_{2.5}$ concentrations in Chiang Mai Province

$PM_{2.5}$ concentration was measured from two monitoring stations in Chiang Mai province: Yupparaj Wittayalai Station (36T) and Chiang Mai City Hall (35T). These stations provide hourly $PM_{2.5}$ concentration data associated with other applicable meteorological data, including temperature, relative humidity, wind speed, and wind direction. Chiang Mai Province has significant levels of air pollution for a few months of the year, ranking it among the world's most polluted cities (IQAirNews, 2021). The primary cause of air pollution is agricultural burning, which is the process of setting fire to cultivated fields in order to prepare the ground for the subsequent crop, most often sugarcane, rice, or maize. Between December and April, these burns take place. During these hours, air quality exceeds the WHO limit. During burning months, the average $PM_{2.5}$ concentration might approach 400 $\mu g/m^3$ (IQAirNews, 2021.).

This study used data from 2020 to create a high resolution AOD for estimating $PM_{2.5}$ concentration. The highest $PM_{2.5}$ concentration in 2020 from 35T and 36T monitoring stations were 468 $\mu g/m^3$ on March 20 and 285 $\mu g/m^3$ on March 20, respectively. During the months of February and April, the 24-hr concentration of $PM_{2.5}$ exceeded the Standard level of 50 $\mu g/m^3$ for many days which during the agricultural burning season. For other months, the concentration was lower than the ambient air quality standard. Figure 4.1 indicates the daily trend of $PM_{2.5}$ concentrations from two Chiang Mai air monitoring stations for 2020.

For hourly concentration during a day, the concentration was higher in the morning than the concentration in the evening, and these changes depend on the burning time of their agricultural residues. There were 70 days in 2020 that the daily average $PM_{2.5}$ concentration was above the national ambient air quality standard vales. From Yupparaj Wittayalai Station (36T), totally 69 days, the concentration was above the standard level.

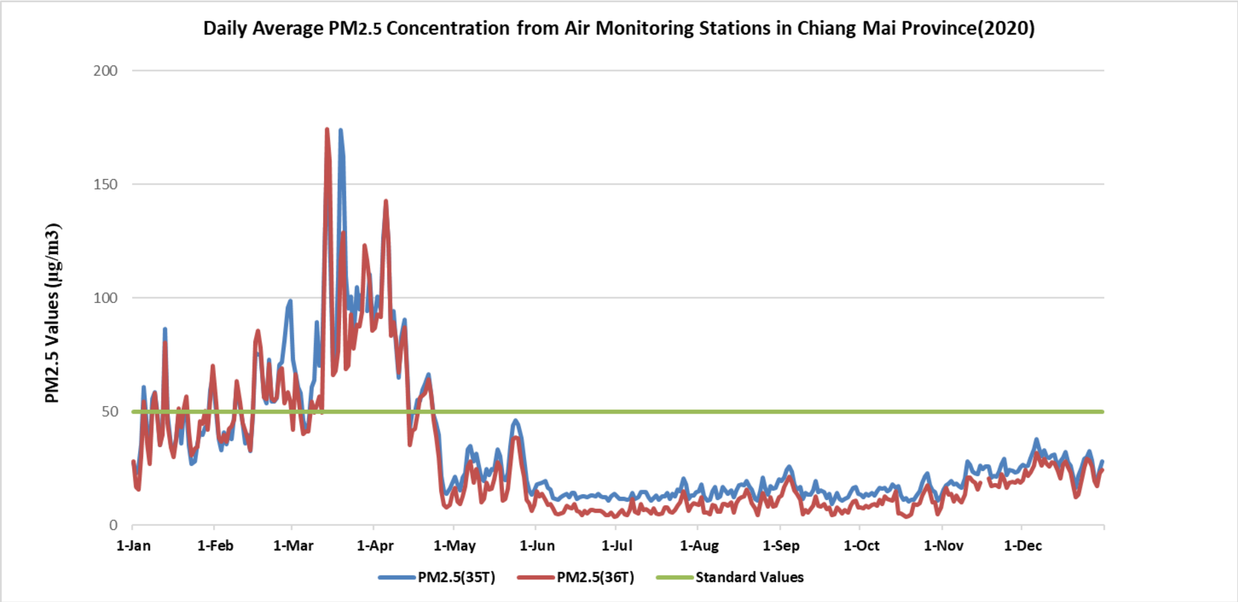

Figure 4.1: Daily average $PM_{2.5}$ concentration from two Chiang Mai Air Monitoring Stations in 2020

4.1.2 AERONET Data

In Chiang Mai Province, there is only one AERONET sun photometer station which provides AOD data. AOD products from this station were used to validate AOD from satellites. Data were collected based on the study period of 2020, and the values of AOD from AERONET were found higher in the dry season than in the wet season of 2020. Although AERONET AOD values were available with high temporal resolution from January to December, there were many missing data during February to May due to sensor error and cloud cover. Figure 4.2 shows the time series of AOD from Chiang Mai AERONET Station during 2020. In this study, AOD from AERONET station were used to validate the AOD from two different satellite.

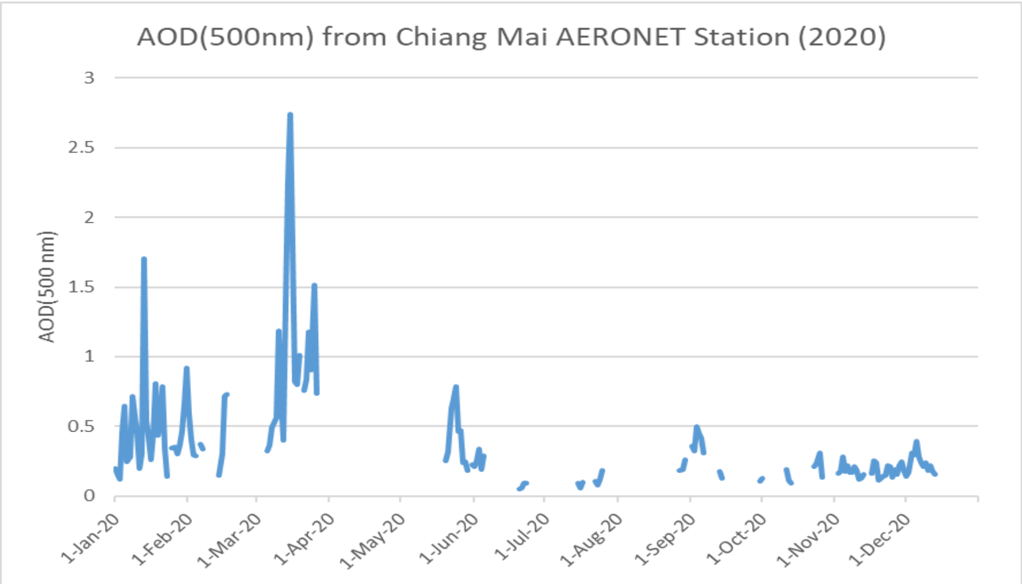

Figure 4.2: AOD Data from Chiang Mai AERONET Station in 2020

4.2 Development of Hourly 1km^2 Resolution AOD

In this study, AOD Products from two separate satellites were combined to achieve high spatial and temporal resolution. The MAIAC AOD from the MODIS sensor can offer high spatial resolution data, while the Hamawari-8 provides hourly AOD products with a spatial resolution of 5 x 5 km^2. In the year of 2020, AOD values from both satellites were not available especially during wet season, and there were missing data during the wet season from June to November. Figure 4.3 shows the distribution of monthly AOD from Himawari-8 satellites over Chiang Mai Province during the study year. In distribution maps, AOD values from February to May were higher than other months.

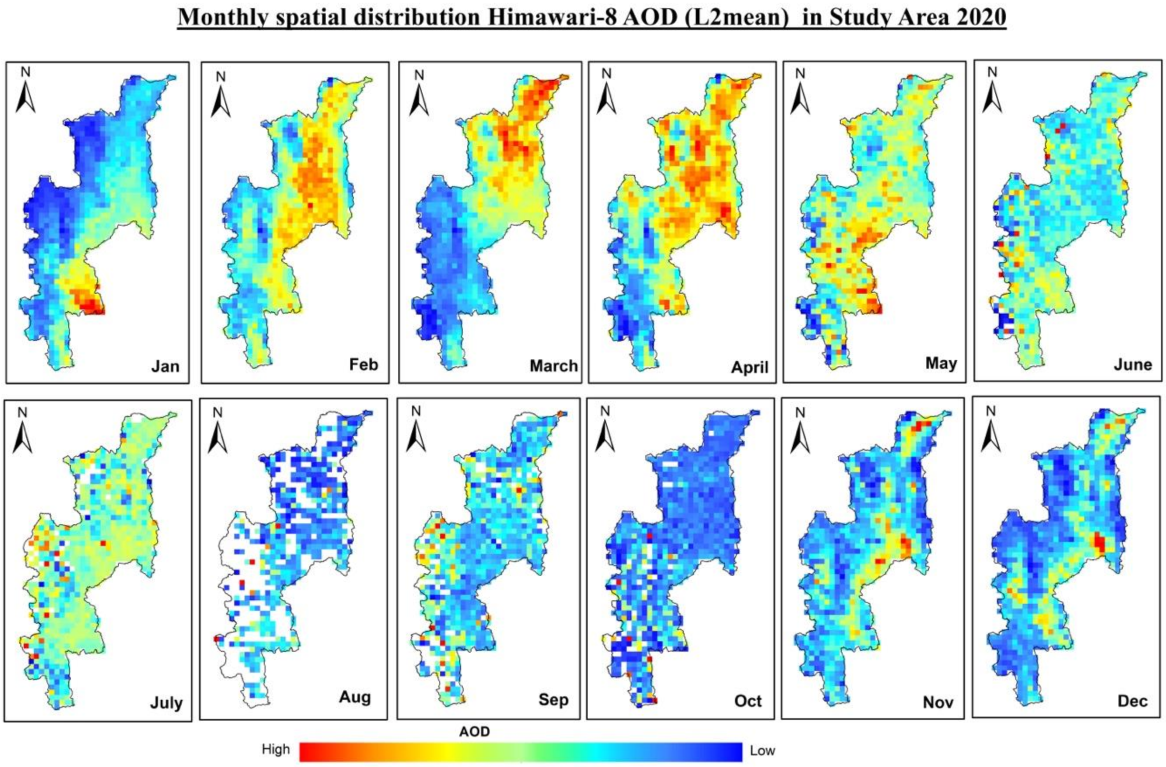

Figure 4.3: Monthly AOD Data from Himawari-8 over study area in 2020

4.2.1 Downscaling Himawari-8 AOD products

Hourly AOD from Himawari-8 with 5km^2 spatial resolution were downscaled to the same resolution as MAIAC AOD (1km^2). Resampling approach in ArcGIS was applied in this procedure. During the year 2020, there were some AOD that were not recorded because of cloud cover and unanticipated sensor error. The images below show the output of downscaling Himawari-8 AOD to a resolution of 1x1 km^2. The correlation coefficient between MAIAC and downscaled Himawari-8 AOD were resulted with higher relation during from January to April 2020.

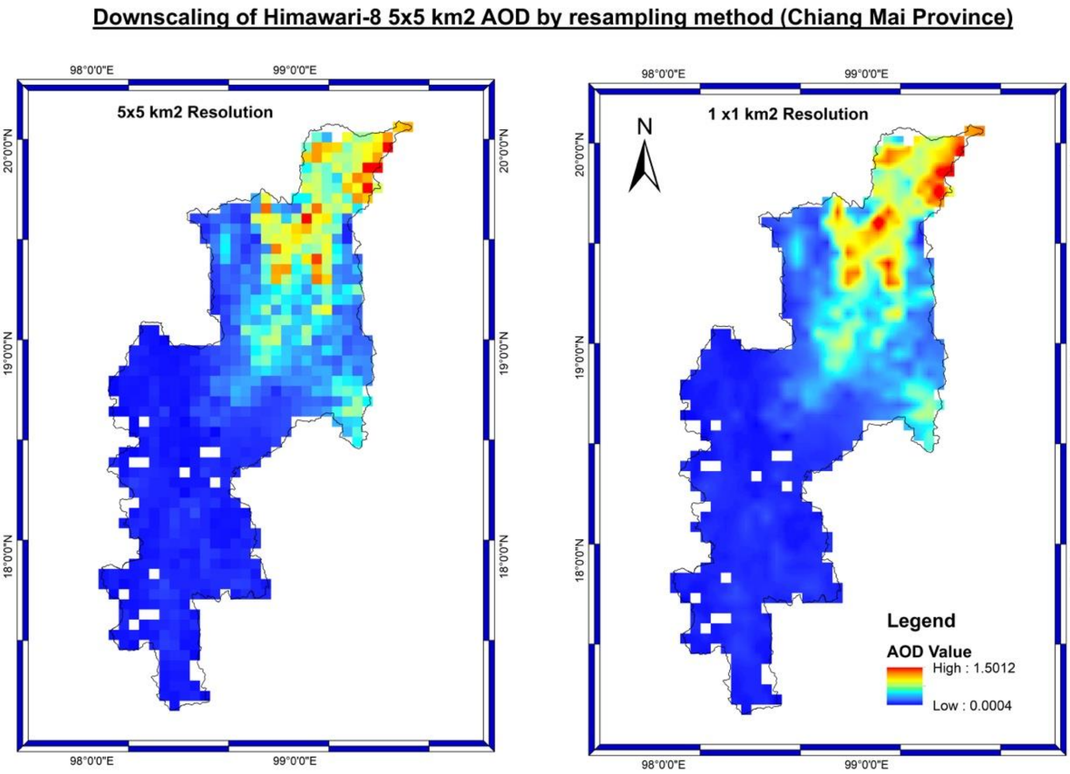

Figure 4.4: Downscaling to 1x1 km^2 by resample method

The following Table 4.1 shows the result of R^2 of two different AOD products.

Table 4.1: Summary of Correlation Results between MAIAC and Himawari-8

	January	February	March	April
Time		R Squared		
9:00	0.33	0.48	0.71	0.10
10:00	0.63	0.62	0.64	0.46
11:00	0.72	0.65	0.82	0.73
12:00	0.52	0.68	0.64	0.82
13:00	0.36	0.50	0.40	0.74
14:00	0.32	0.40	0.20	0.62
15:00	0.18	0.30	0.14	0.45
16:00	0.19	0.06	0.11	0.17

After downscaling Himawari-8 AOD with 5x5 km^2 resolution, AOD products from MAIAC and Himawari-8 were integrated by linear regression (LR) to develop hourly 1x1km^2 resolution AOD for the estimation of $PM_{2.5}$ concentration.

Then, the linear regression was used to develop the relationship in each hour from 09:00 to 16:00 hr. with MAIAC AOD values derived from averaging Terra (10:00 hr.) and Aqua (13:00 hr.). The following equations were used to develop hourly high spatial resolution

AOD of Himawari-8 at 1x1km^2 AOD by the use of raster calculator under Math Algebra tools of ArcMap.

$$MAIAC\ AOD = (0.4733 \times Himawari\text{-}8\ AOD_{09:00}) - 0.008$$

$$MAIAC\ AOD = (2.5561 \times Himawari\text{-}8\ AOD_{10:00}) - 0.1586$$

$$MAIAC\ AOD = (1.8221 \times Himawari\text{-}8\ AOD_{11:00}) - 0.009$$

$$MAIAC\ AOD = (1.0864 \times Himawari\text{-}8\ AOD_{12:00}) + 0.0629$$

$$MAIAC\ AOD = (0.7982 \times Himawari\text{-}8\ AOD_{13:00}) + 0.1004$$

$$MAIAC\ AOD = (0.6336 \times Himawari\text{-}8\ AOD_{14:00}) + 0.116$$

$$MAIAC\ AOD = (0.6429 \times Himawari\text{-}8\ AOD_{15:00}) + 0.1185$$

$$MAIAC\ AOD = (0.6407 \times Himawari\text{-}8\ AOD_{16:00}) + 0.09$$

Figure 4.4 shows the spatial distribution of high resolution AOD generated from different satellites on April 6, 2020.

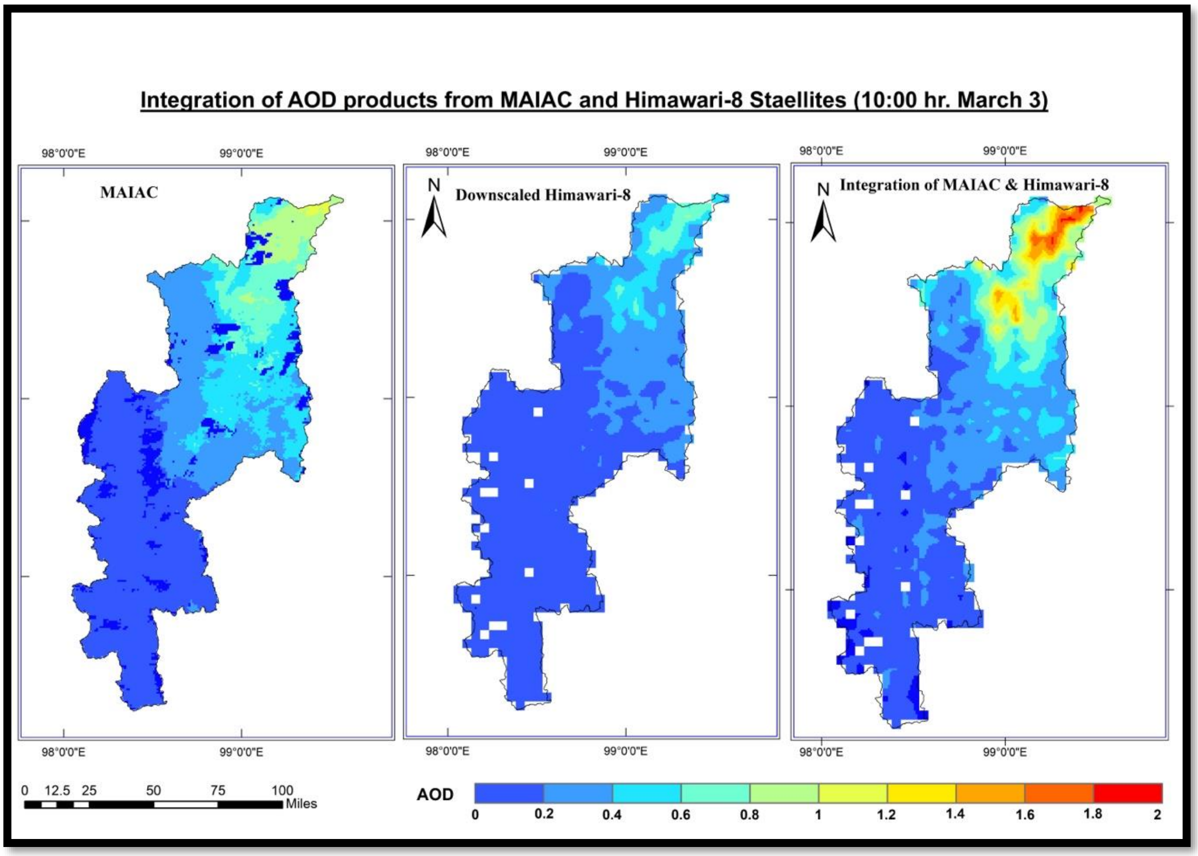

Figure 4.5: Integration of AOD from two different satellites

Spatial distribution of hourly 1x1 km^2 resolution AOD over the Chiang Mai province showed that the AOD values were available in morning time from 09:00 to 12:00 hr. and there were many missing data in afternoon especially during 15:00 and 16:00 hr. due to the imagery time of Himawari-8 satellites for Chiang Mai province area. Figure 4.6 shows the AOD distribution over the study area during March 2020. The AOD values were higher in Northern part of the study area in every hour.

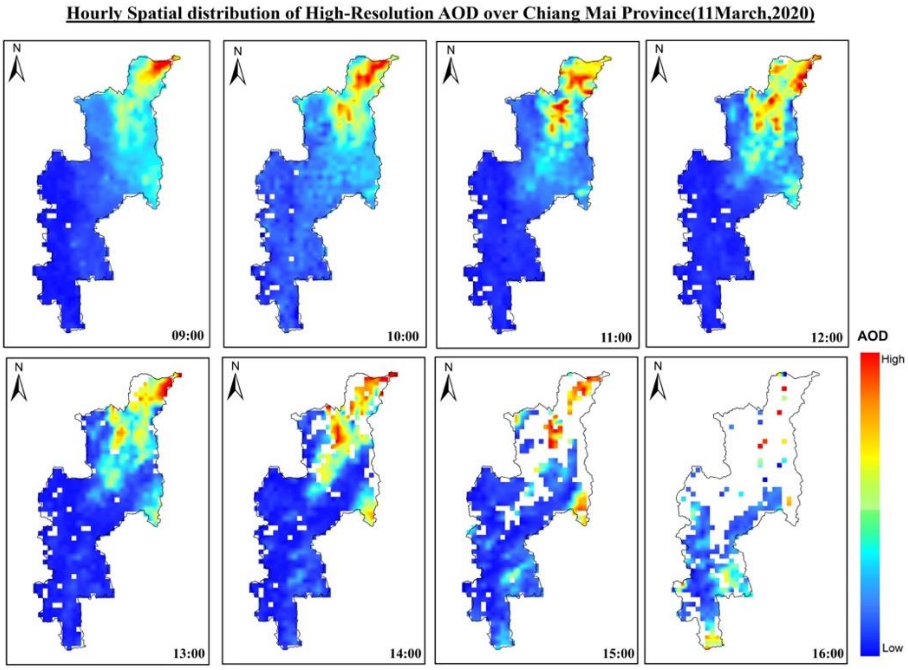

Figure 4.6: spatial distribution of high resolution AOD

4.3 Validation of High Resolution AOD with AERONET Station

High resolution AOD derived from MAIAC and Himawari-8 was validated using AERONET's AOD of Chiang Mai station during studying time 2020. The result shows that AOD from MAIAC and Himawari-8 had correlation coefficient (R squared) as 0.63 with AERONET's AOD during 2020. AOD from MAIAC with 1x 1 km^2 resolution was also applied to compare with high temporal and spatial AOD from integration of two satellite products. The correlation coefficient between AERONET and MAIAC was R^2 0.66. The R squared result from MAIAC has slightly higher correlation with AERONET's AOD because MAIAC's AOD has 1x1 km^2 spatial resolution, and it was generated from averaging AOD from MODIS Terra and Aqua. The evaluation between satellite AOD and AERONET's was conducted with averaged AOD from 10:00hr and 13:00 hr. at which Terra and Aqua passed over the study area. Hourly integrated AOD from two satellites had slightly lower R^2 result with AERONET because the evaluation was applied each hour from 09:00 hr. to 16:00 hr. and AODs from Himawari-8 were unavailable especially during afternoon time. Figure 4.7 shows comparison of relationship between AOD from AERONET station and High Resolution AOD from MAIAC and Himawari-8.

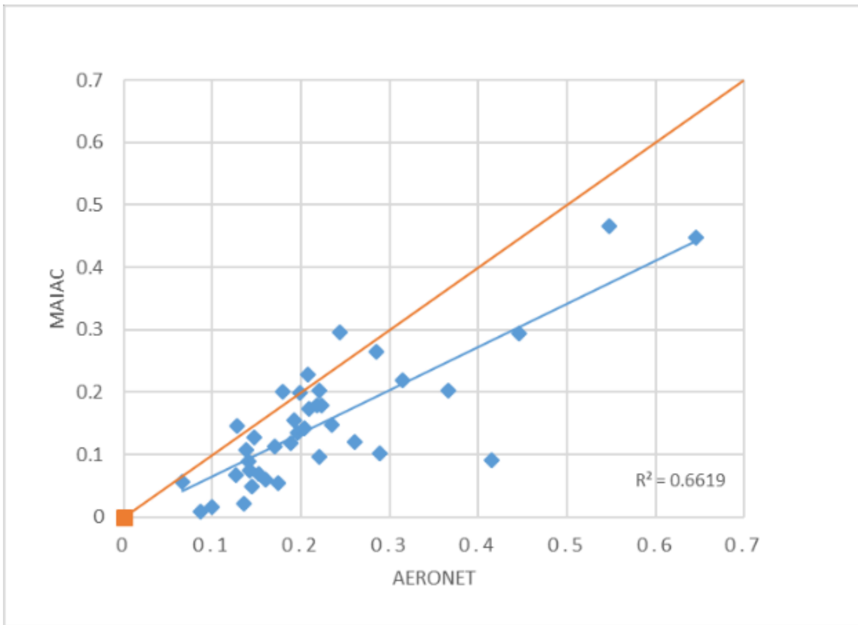

(a)

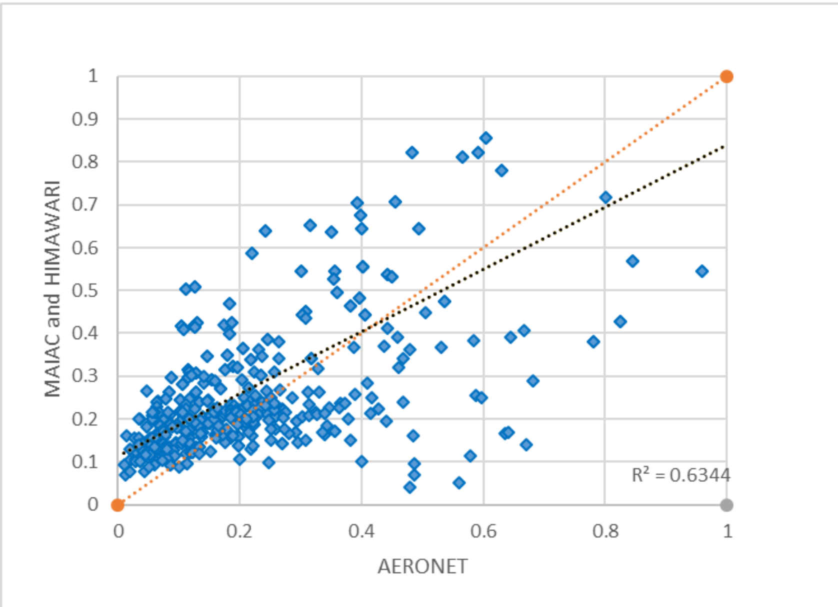

(b)

Figure 4.7: Comparison of relationship between AOD from AERONET station and High Resolution AOD from MAIAC(a) and Himawari-8(b)

Table 4.2: Comparison of Correlation Results from MAIAC and Himawari+MAIAC

	R^2	MAE	RMSE
MAIAC	0.6619	0.08	0.102
Himawari-8+ MAIAC	0.6344	0.132	0.174

The mean difference of satellite AOD and AERONET's AOD was presented as mean absolute error MAE 0.132 and root mean squared error RMSE 0.174 with the 446 number of observations. According to the validation results obtained with AERONTE AOD from Chiang Mai, the performance of the high-resolution downscaling Himawari-8 satellite AOD was within acceptable limits with R^2 0.63.

4.4 Hourly Relationship between AOD and $PM_{2.5}$ Concentration

In this process, the relationship between AOD and $PM_{2.5}$ concentration was estimated from 1hour average value of $PM_{2.5}$ concentration from two air monitoring stations in Chiang Mai and an hourly AOD from high-resolution Himawari-8 AOD by using multiple Linear Regression. $PM_{2.5}$ data and AOD were separated into 70% and 30% for training and testing sets. These datasets were randomly selected from all of data of study period. 70% of data were used to develop the relationship and 30% of data were applied for the validation the result from regression. The linear regression equation between AOD and $PM_{2.5}$ concentrations without adding meteorological parameters resulted in the correlation coefficient R^2 of 0.56. After adding meteorological parameters of temperature, relative humidity, wind speed, and wind direction, the value of R squared was increased to 0.62.

Table 4.3: Relationship between AOD and $PM_{2.5}$

Model	Independent variables	N	R	R^2	Equation
1	AOD	1015	0.752	0.566	$PM_{2.5}$= 19.38 +80.93 AOD
2	AOD, Temp, RH, WS, WD	1015	0.791	0.626	$PM_{2.5}$= 144.48 +79.87 AOD – 2.503Temp – 0.95 RH – 5.83 WS – 0.02 WD

Figure 4.8 shows the correlation result of AOD and $PM_{2.5}$ in the training and testing sets. The R squared of training set was 0.55, and the R square for the testing set was 0.58. This result is from the model between high resolution AOD and $PM_{2.5}$ concentration without meteorological parameters.

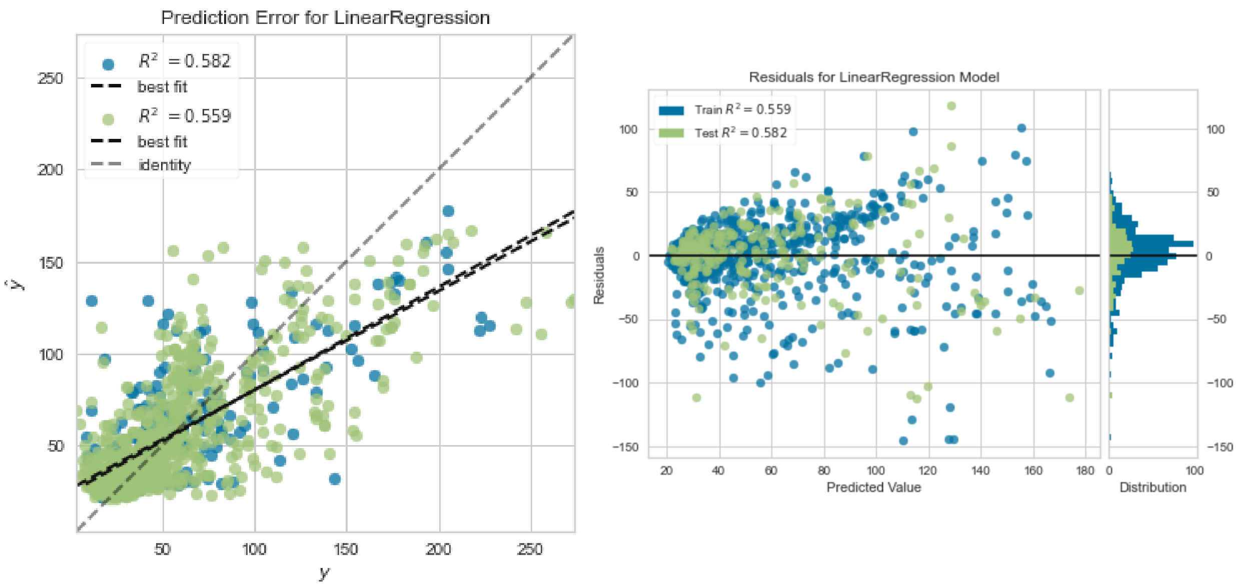

Figure 4.8: Results from Linear regression of AOD and $PM_{2.5}$

The result of relationship between hourly AOD and $PM_{2.5}$ concentration with meteorological data showed that the R squared of the training set was 0.650, and the R-square of the testing set was 0.576. The correlation between AOD and $PM_{2.5}$ with meteorological data are illustrated in Figure 4.9.

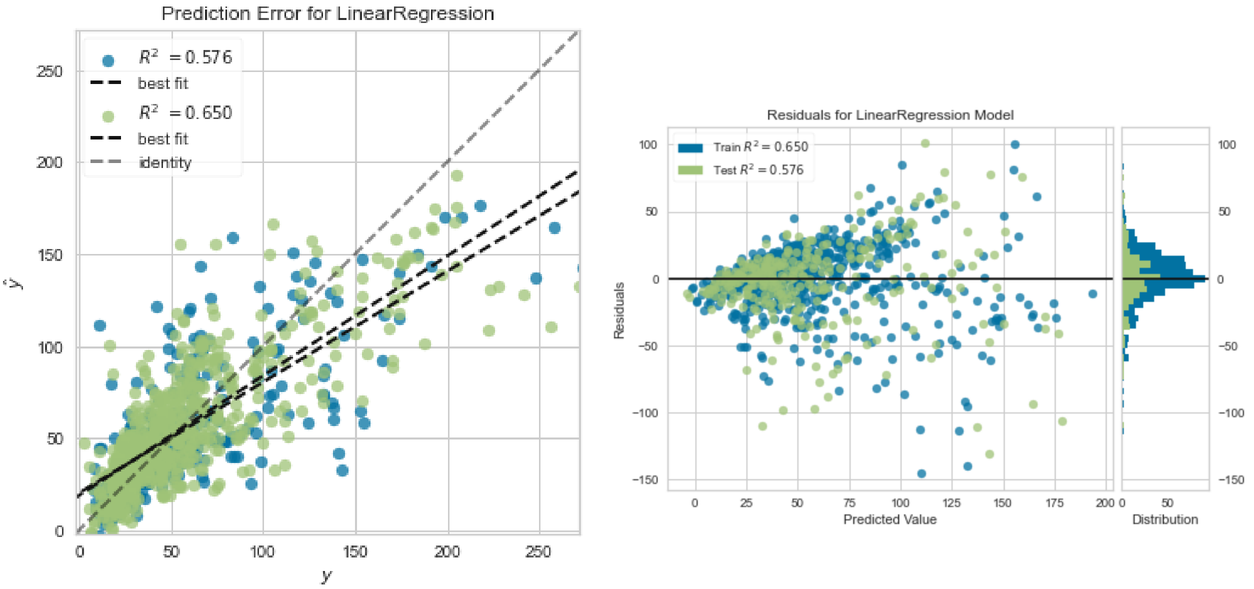

Figure 4.9: Results from Linear regression of AOD and $PM_{2.5}$ with Meteorological data

For comparison, Random Forest Regression (RFR) was also applied in this study. RFR used AOD and other meteorological parameters to estimate $PM_{2.5}$ concentration for the study area. The Random Forest Regression result showed that training set had RMSE as 9.91, and the R-square as 0.94 while the testing set has RMSE as 28.76 and R-square as 0.5296.

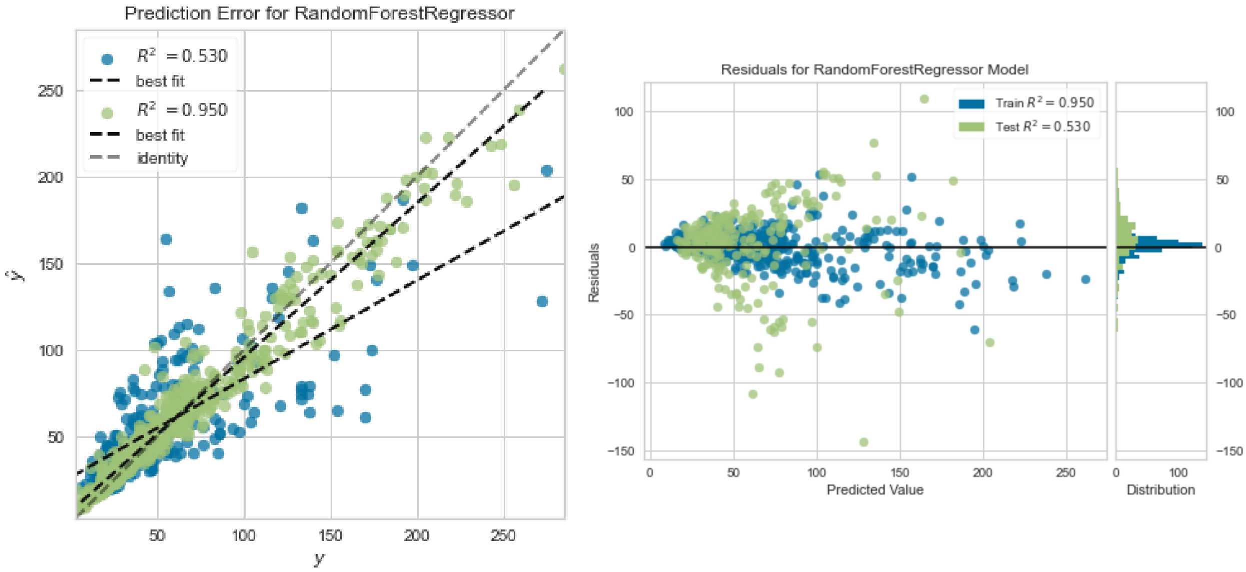

Figure 4.10: Results from Random Forest regression of AOD and $PM_{2.5}$ with Meteorological data

According to the result from Random Forest Regression, Aerosol Optical Depth is the highest variable importance to compare with other variables. Wind Speed was the lowest feature with $PM_{2.5}$ estimation.

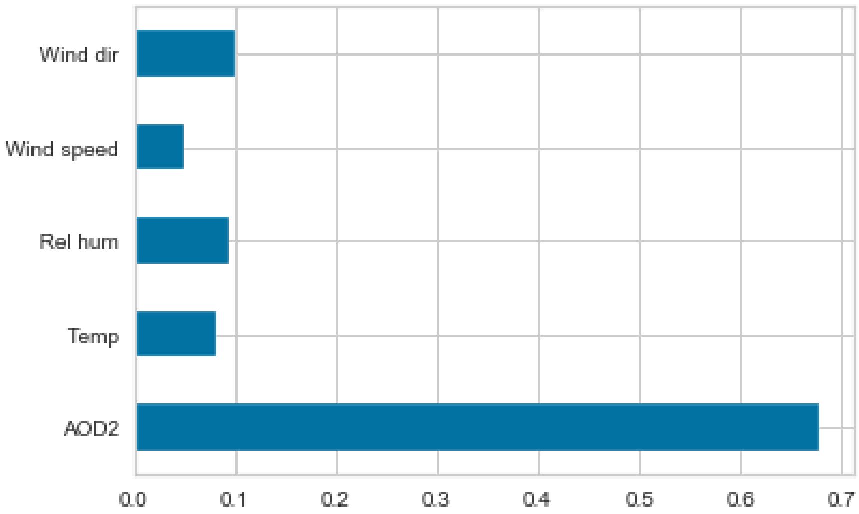

Figure 4.11: Variable Importance results from Random Forest Regression

4.5 Evaluation of the Hourly $PM_{2.5}$ Model

The model for $PM_{2.5}$ concentration estimation was tested against the actual $PM_{2.5}$ concentration from the concentration from the two air quality monitoring stations in Chiang Mai. The meteorological data were averaged for hourly data from 09:00 to 16:00 hr. provided from two air quality monitoring station in Chiang Mai. Equation 4.1 was developed to estimate $PM_{2.5}$ concentration from the high-resolution satellite derived AOD with meteorological parameters, respectively.

$$PM_{2.5} = 144.48 + 79.887AOD - 2.503Temp - 0.959RH - 5.837WS - 0.026WD \qquad \text{(Eq 4.1)}$$

Where: AOD: Aerosol Optical Depth
Temp: Temperature(°C)
RH: Relative Humidity (%)
WS: Wind Speed (m/s)
WD: Wind Direction (Degree)

The summary of hourly correlation results between the estimated $PM_{2.5}$ concentration and observed $PM_{2.5}$ values are illustrated in Table 4.3. The correlation coefficient between observed $PM_{2.5}$ and estimated $PM_{2.5}$ concentration was the highest at 10:00 AM with RMSE of 23.838 and MAE of 16.626. The correlation coefficient of observed $PM_{2.5}$ and estimated $PM_{2.5}$ concentration resulted from the model was 0.715 with RMSE 23.284 µg/m^3. The mean values with standard deviation of observed $PM_{2.5}$ and estimated $PM_{2.5}$ during study period were 55.32± 43.62 µg/m^3 and 56.34± 36.47 µg/m^3, respectively. Figure 4.12 shows the relationship between observed and estimated $PM_{2.5}$ concentration of air monitoring stations in Chiang Mai for the year 2020.

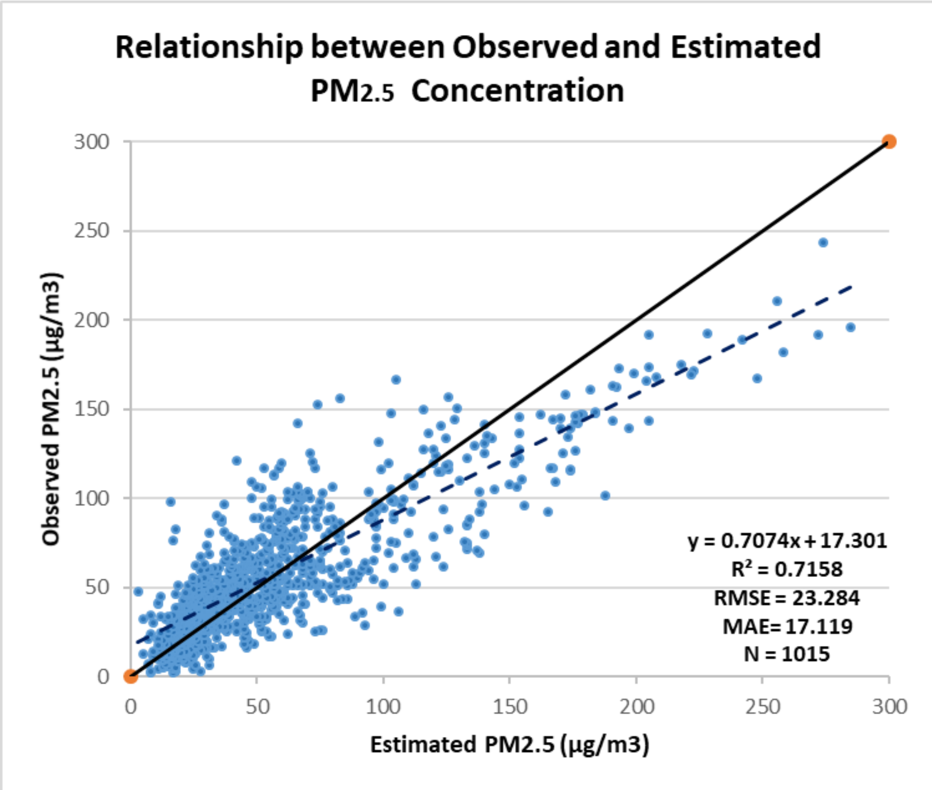

Figure 4.12: The relationship between observed and estimated $PM_{2.5}$ Concentration in Chiang Mai Province

This regression line graph shows the relationship between Estimated $PM_{2.5}$ concentration generated from Multiple linear Regression model and Observed $PM_{2.5}$ concentration from Chiang Mai monitoring Stations during 2020. The correlation result from model was quite good for all observed data with R^2 0.715. With the hourly estimation, R^2 values were higher in morning time (R^2~0.8) than in the afternoon (R^2~0.6)

Table 4.4: Summary of Hourly Correlation Results Observed and Estimated $PM_{2.5}$ Concentration

Time	Observation(N)	R square	RMSE	MAE	Bias
9:00	142	0.77	23.483	17.782	-7.965
10:00	155	0.80	23.838	16.626	-5.581
11:00	153	0.78	24.523	17.314	-3.026
12:00	129	0.69	25.714	18.767	2.734
13:00	123	0.71	23.277	17.944	4.073
14:00	118	0.55	23.869	17.034	5.627
15:00	117	0.65	19.189	14.863	8.316
16:00	77	0.61	19.443	15.974	14.234

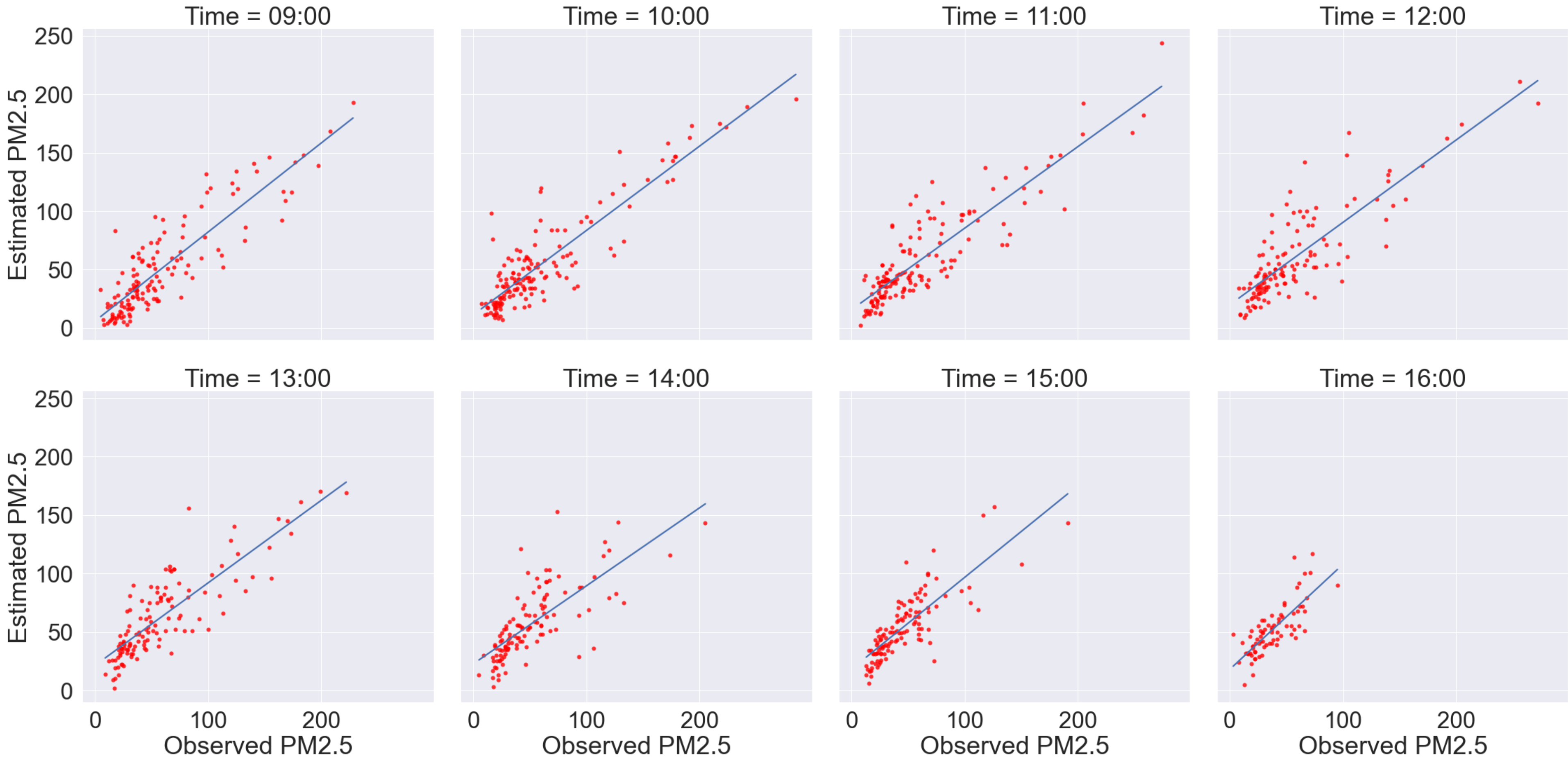

Figure 4.13: Hourly correlation between Observed $PM_{2.5}$ and Estimated $PM_{2.5}$

4.6 Development of Hourly 1x1km^2 Spatial Resolution maps of $PM_{2.5}$ in Chiang Mai

In this part, hourly distribution maps of ground-based $PM_{2.5}$ concentrations over the research area were created from 9:00 to 16:00 hr. $PM_{2.5}$ concentration maps were developed from the MLR model which was include AOD and meteorological parameters. In this process, MLR model based on equation 4.1 and High resolution AOD was applied by raster calculator under math algebra tools in ArcMap to develop hourly maps which have 1x1km^2 spatial resolution.

On April 6, 2020, Figure 4.14 illustrates the hourly geographical distribution of $PM_{2.5}$ concentrations using a data series covering the hours of 9:00 to 16:00. $PM_{2.5}$ concentrations were found to be highest between 9:00 and 12:00 a.m. In overall, AOD measurements were unavailable in the afternoon, resulting in data gaps in Chiang Mai Province. The highest $PM_{2.5}$ concentration was 92.4 µg/m^3 at 10:00 hr. and the lowest values was 22.1 µg/m^{3}at 12:00 on April 6, 2020.

Figure 4.14 to 4.17 illustrate the hourly spatial distribution of $PM_{2.5}$ concentrations using a data series covering the hours of 9:00 to 16:00 during dry season from January to April. In overall, AOD measurements were unavailable in the afternoon, resulting in data gaps in Chiang Mai. During March 11 in 2020, $PM_{2.5}$ concentrations reached higher level (~200µg/m^3) in the northern part of the province. The concentrations were higher in dry season from January to April than the wet season because most of agricultural open burning and forest fires usually occurred in dry season.

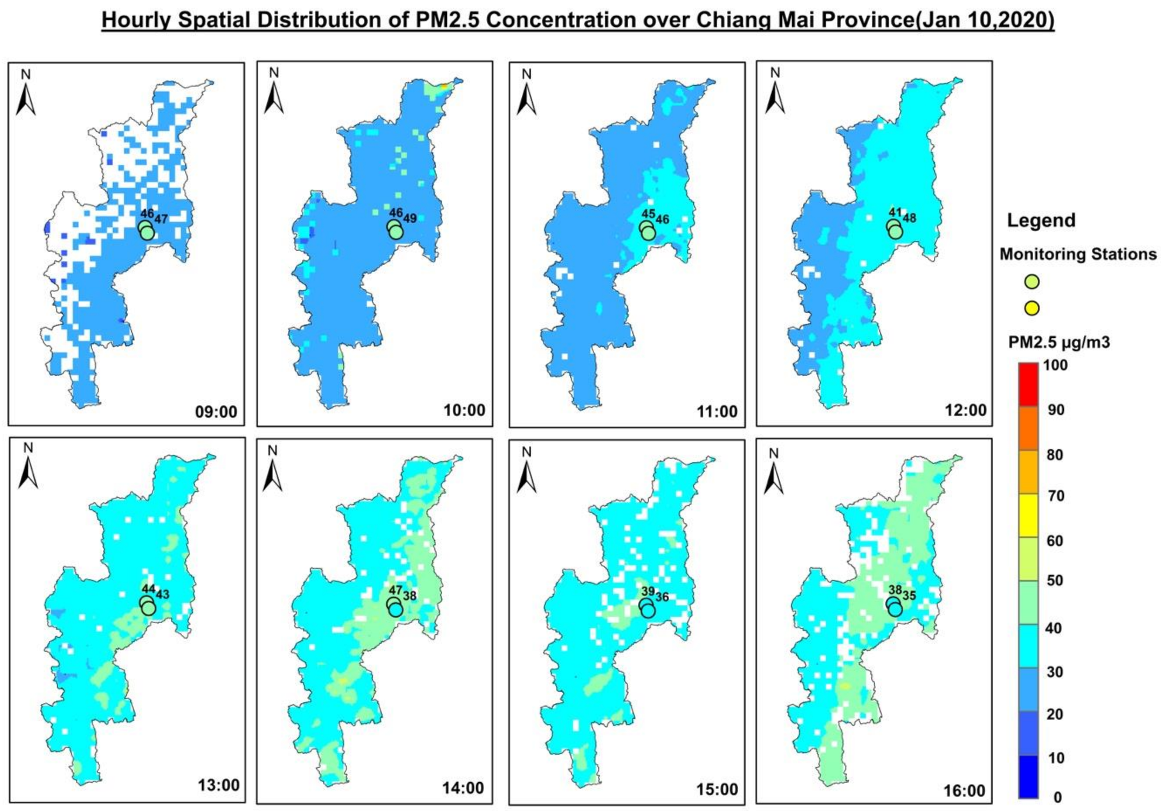

Figure 4.14: Hourly Spatial distribution of $PM_{2.5}$ concentration Maps with (1x1km^2) resolution over Chiang Mai Province (January)

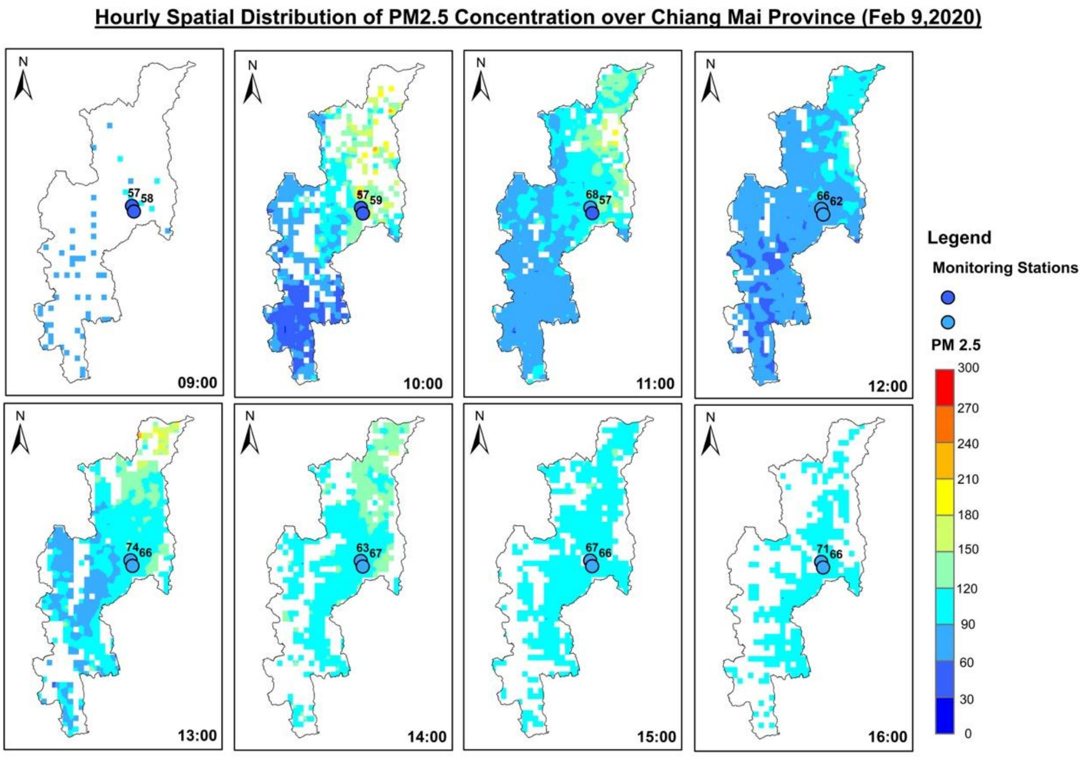

Figure 4.15: Hourly Spatial distribution of PM2.5 concentration Maps with (1x1km^2) resolution over Chiang Mai Province (February)

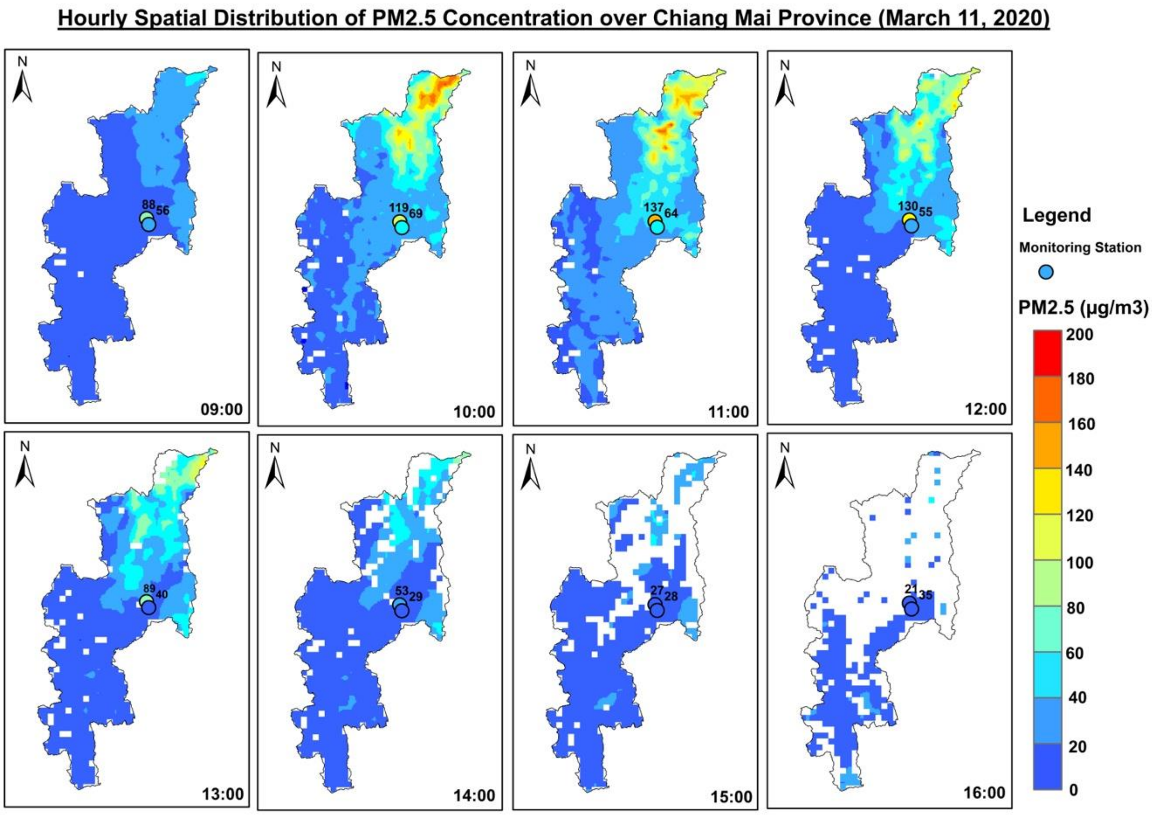

Figure 4.16: Hourly Spatial distribution of PM2.5 concentration Maps with (1x1km^2) resolution over Chiang Mai Province (March)

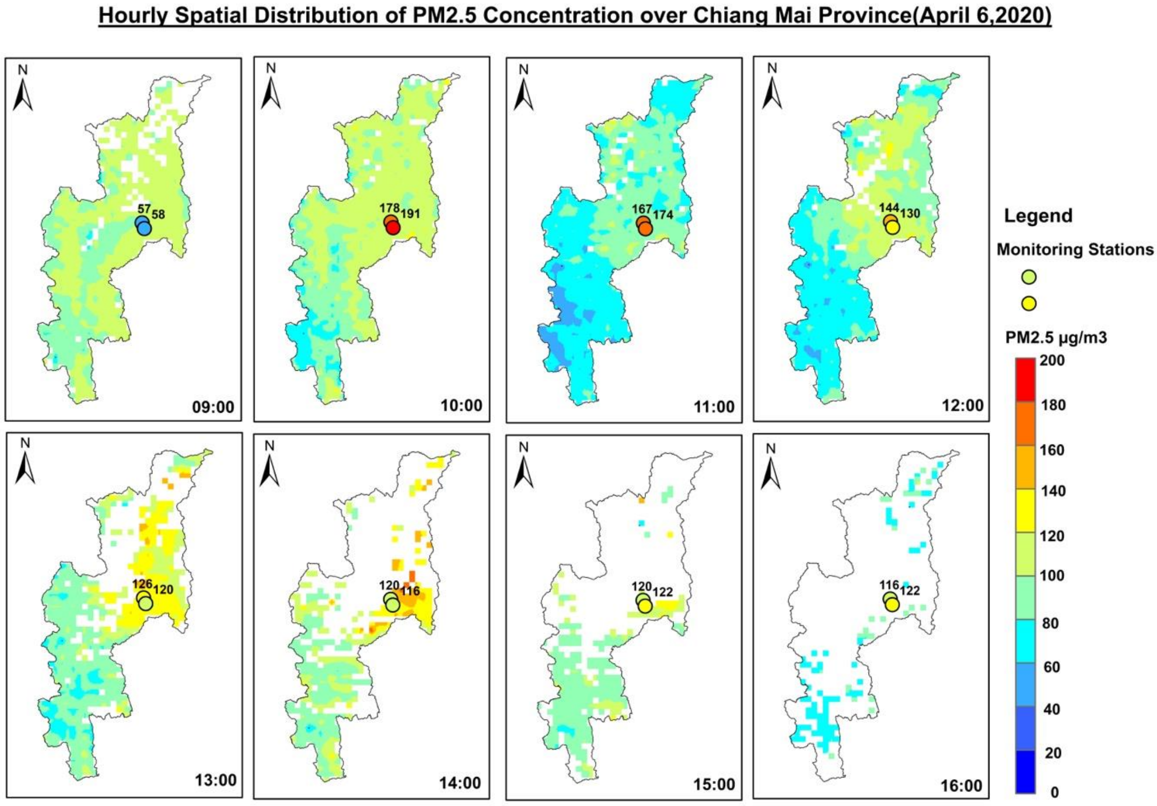

Figure 4.17: Hourly Spatial distribution of $PM_{2.5}$ concentration Maps with ($1x1km^2$) resolution over Chiang Mai Province (April)

Chapter 5

Conclusions and Recommendations

The primary purpose of this research was to estimate $PM_{2.5}$ concentrations using high temporal and spatial resolution AOD which were developed from two separate satellites, MAIAC and Himawari-8, with meteorological factors. The spatial resolution was 1 x 1km^2 and the time resolution was hourly. The study area was Chiang Mai Province, which is located in northern Thailand and is vulnerable to air pollution, particularly during the dry season.

The Multiple Linear Regression model with AOD and meteorological parameters was used to generate the equation to estimate $PM_{2.5}$ concentration. To compare the output of results, the Random Forest Regression approach was also used. Both strategies produced nearly identical results, with R^2 of 0.73 in the training set and0.71 in the testing set.

5.1 Conclusion

1. The hourly $PM_{2.5}$ concentration from two air quality monitoring stations in Chiang Mai Province during 2020 were collected. The maximum concentration from Chiang Mai City Hall station (35T) and Yupparaj Wittayalai Station (35T) was found in March 20 and 19, respectively. $PM_{2.5}$ concentration in Dry season months (January to April) reached the high level above the national ambient air quality standard value of 50 µg/m^3 for 24 hours.

2. Hourly 1x1 km^2 spatial resolution AOD products derived from MAIAC and Himawari-8 were validated with ground-based AERONET's AOD from Chiang Mai Station. The result showed that the relationship between Satellite AOD and AERONET's AOD has R^2 of 0.63 and RMSE of 0.17.

3. Estimation of $PM_{2.5}$ concentration conducted by using satellite AOD and meteorological parameter at the same location of air quality monitoring stations in Chiang Mai during 9:00 to 16:00 hrs. Hourly average meteorological parameters was done by using the multiple linear regression. Five parameters involved in the linear regression were AOD, Temperature, wind speed, and wind direction. The model result showed a good performance with the observation data with the correlation coefficient (R^2) of 0.65.

4. Using the same independent variables, random forest regression was also utilized to estimate $PM_{2.5}$ concentrations. The R^2 was 0.95 with a root mean square error of 9.92 in the training set and R^2 of 0.53 with a root mean square error of 28.76 in the testing set.

5. The model's performance was tested using 1-hour-average $PM_{2.5}$ concentrations from two air monitoring sites in Chiang Mai province between 09:00 and 16:00 local time. Overall, the predicted $PM_{2.5}$ concentrations coincided well with a R^2 of 0.71, while the MAE and RMSE were 17.119 and 23.284 µg/m^3, respectively.

6. During the study period of 2020, an hourly map of $PM_{2.5}$ concentration with 1 x 1 km^2 spatial resolution over Chiang Mai province was developed using the linear regression equation developed from the integration method of MAIAC and

resampled Himawari-8 AOD products, ground station $PM_{2.5}$ concentration, and meteorological data.

5.2 Limitation

There were two main type of limitations in this research regarding the development of hourly $1x1km^2$ spatial resolution AOD from MAIAC and Himawari-8. Satellite image data could not provide all of the AOD data required for the research period and had a significant amount of missing data from cloud cover. This resulted in a decrease in the number of samples necessary for the analysis.

The second limitation is accessibility of data sources on the ground. The number and locations of monitoring stations of $PM_{2.5}$ and meteorological data were largely limited. Chiang Mai province currently has just one AERONET station for validation with satellite AOD, and additional stations are required to ensure data accuracy. Air monitoring stations in Chiang Mai are positioned quite close together, and data from these stations cannot be used to monitor the entire area's air quality.

5.3 Recommendation

High resolution AOD from the MAIAC and Himawari-8 satellites can be used to estimate $PM_{2.5}$ concentrations in the studied area. However, Chiang Mai has relatively limited options for installing air quality monitoring stations, and these places have a wide range of terrain conditions, resulting in a wide range of climate conditions. As a result, there may be a high level of uncertainty in the model's estimation of $PM_{2.5}$ concentrations at other places.

Recommendations are as follows:

1. To construct a more realistic model, study sites with additional ground-based air quality monitoring stations should be used. In order to collect more data for validation, low-cost PM sensors should be deployed.

2. This study only covered 2020, and there were a lot of missing AOD data from AERONET's AOD and satellite data during that year. To achieve good model performance, the study period should be chosen based on data availability. To obtain a wider range of $PM_{2.5}$ estimation for different years, the research time should be extended.

3. This study only focused on downscaled Himawari-8 AOD $1km^2$ resolution to estimate $PM_{2.5}$ concentration. AOD data from the original resolution $5km^2$ need to be also applied to analyze similarity by the comparison of before and after downscaling.

4. The model only employed four different types of meteorological characteristics derived from the same air monitoring stations. Because $PM_{2.5}$ concentrations are strongly related to meteorological conditions, the overall meteorological data collected from each grid of the study sites should be used to improve model performance.

5. This study was based on the year of 2020 from January to December. The model performance needs to be compared with the same time series in different year. Therefore, different study years such as from 2018 to 2021 should be applied in order to compared the prediction results and improve the prediction efficiency for the same months in each year.

6. There is just one ground-based AERONET station using solar photometers in Chiang Mai for validation with satellite AOD. To achieve high accuracy, additional AERONET stations with proper calibration and maintenance need be installed.

7. Estimation model from this study was based on the ground-based data from monitoring stations and AODs from satellites. $PM_{2.5}$ concentrations may be altered with other factors such as topography, land use type, and climatic condition. For other area, more additional data should be applied to get the high accuracy.

8. According to the findings, data availability is a critical aspect in the development of high-accuracy, high-performance $PM_{2.5}$ estimation. Other sources of satellite-derived AOD with high spatial and temporal resolution should be used to compare the result of this research and earlier studies.

References

Archer D., Nikam J., & Nopsret C. (2021). *Air quality in Thailand: Understanding the regulatory context*, Stockholm Environment Institute.

Bhaskaran, S., Phillip, N., Rahman, A., & Mallick, J. (2011). Applications of Satellite Data for Aerosol Optical Depth (AOD) Retrievals and Validation with AERONET Data. In *Atmospheric and Climate Sciences*, *01*(02)61–67. https://doi.org/10.4236/acs.2011.12007

Bilal, M., Nichol, J. E., Bleiweiss, M. P., & Dubois, D. (2013). A Simplified high resolution MODIS aerosol retrieval algorithm (SARA) for use over mixed surfaces. *Remote Sensing of Environment*, *136*,135-145.https://doi.org/10.1016/j.rse.2013.04.014

Borra, S., Thanki, R., & Dey, N. (2019). *Satellite image analysis : Clustering and classification.* https://doi.org/10.1007/978-981-13-6424-2

Chu, Y., Liu, Y., Li, X., Liu, Z., Lu, H., Lu, Y., Mao, Z., Chen, X., Li, N., Ren, M., Liu, F., Tian, L., Zhu, Z., & Xiang, H. (2016). A review on predicting ground $PM_{2.5}$ concentration using satellite aerosol optical depth. *Atmosphere*, *7*(10), 1–25. https://doi.org/10.3390/atmos7100129

Dayou, J., Chang, J. H. W., & Sentian, J. (2014). Ground-based aerosol optical depth measurement using sunphotometers. *SpringerBriefs in Applied Sciences and Technology*, (9-30). https://doi.org/10.1007/978-981-287-101-5

Filonchyk, M., Yan, H., Zhang, Z., Yang, S., Li, W., & Li, Y. (2019). Author Correction: Combined use of satellite and surface observations to study aerosol optical depth in different egions of China. *Scientific Reports*, *9*(1), 1–15. https://doi.org/10.1038/s41598-019-54734-6

IQAir. (2020).*World Air Quality Report*, (pp. 1–35). https://www.iqair.com/world-most-polluted-cities/world-air-quality-report-2019en.pdf

Janjai, S., Nunez, M., Masiri, I., Wattan, R., Buntoung, S., Jantarach, T., & Promsen, W. (2012). Aerosol optical properties at four sites in Thailand. *Atmospheric and Climate Sciences*, *02*(04), 441–453. https://doi.org/10.4236/acs.2012.24038

Jansakoo, T. (2020). *Estimation of high-resolution fine particulate matter concentration in Bangkok Metropolitan Region using satellite-derived aerosol optical depth, land-use and meteorologica parameters*. (Master Thesis No. EV-20-12, Asian Institute of Technology, 2020). Bangkok: Asian Institute of Technology.

Jessica, C., John, S., & Chay, T. (2012). Particulate Matter (PM) Sources. In *Valley Air District* (p. 1). http://www.valleyair.org/air_quality_plans/AQ_plans_PM_sources.htm

Jin, Y., Hao, Z., Chen, J., He, D., Tian, Q., Mao, Z., & Pan, D. (2021). Retrieval of urban aerosol optical depth from landsat 8 OLI in Nanjing, China. *Remote Sensing*, *13*(3), 1–19. https://doi.org/10.3390/rs13030415

Kanabkaew, T. (2013). Prediction of Hourly Particulate Matter Concentrations in Chiangmai, Thailand Using MODIS Aerosol Optical Depth and Ground-Based Meteorological Data. *EnvironmentAsia. 6,* 65-70. https://doi.org/10.14456/ea.2013.20.

Kouimtzis, T., & Samara, C. (1995). Airborne Particulate Matter. *The Handbook of Environmental Chemistry 4 (*Part D*).*

Kumharn,W., & Pilahome, O. (2019). *Aerosols optical properties based on AERONET and MODIS data in Thailand*. https://www.researchgate.net/publication/337102631

Kusuma, W. L., Chih-Da, W., Yu-Ting, Z., Hapsari, H. H., & Muhamad, J. L. (2019). $PM_{2.5}$ pollutant in asia—a comparison of metropolis cities in indonesia and taiwan. *International Journal of Environmental Research and Public Health*, *16*(24), 1–12. https://doi.org/10.3390/ijerph16244924

LAADS DAAC. (2020). *Moderate Resolution Imaging Spectroradiometer (MODIS) - LAADS DAAC*. *Nasa*. https://modaps.modaps.eosdis.nasa.gov/services/about/products

Lim, H. S., MatJafri, M. Z., Abdullah, K., & Wong, C. J. (2009). Air pollution determination using remote sensing technique, Advances in Geoscience and Remote Sensing, Gary Jedlovec, IntechOpen, http://doi.org/10.5772/8319. https://www.intechopen.com/chapters/9534

Lindstrom, S. (2018). Aerosol Optical Depth Quick Guide. *Cooperative Institute for Meteorological Satellite Studies*, 15–16. http://cimss.ssec.wisc.edu/goes/OCLOFactSheetPDFs/ABIQuickGuide_BaselineAerosolOpticalDepth.pdf

Liu, Y., Paciorek, C. J., & Koutrakis, P. (2009). Estimating regional spatial and temporal variability of $PM_{2.5}$ concentrations using satellite data, meteorology, and land use information. *Environmental Health Perspectives*, *117*(6), 886–892. https://doi.org/10.1289/ehp.0800123

Lyapustin, A., & Wang, Y. (2018). *MODIS Multi-Angle Implementation of Atmospheric Correction (MAIAC) Data User ' s Guide*. *6*(June), 1–19.

National Aeronautics and Space Administration. (2013). *NASA logo*. https://commons.wikimedia.org/wiki/File:NASA_logo.svg

NOAA NESDIS Aerosol Product Application Team. (2012). ABI Suspended Matter/Aerosol Optical Depth and Aerosol Size Parameter. *NOAA NESDIS Center for Satellite Applications and Research Algorithm Theoretical Basis Document*, *3*.

Pollution Control Department (PCD). (2004).*Water Quality Standards*. http://infofile.pcd.go.th/mgt/PollutionReport2015_en.pdf?CFID=2140989&CFTOKEN=61488210%0Ahttp://www.pcd.go.th/%0Ahttp://www.pcd.go.th/info_serv/en_reg_std_water04.html

Pollution Control Department (PCD). (2015). Thailand State of Pollution Report 2015. *PCD No. 06-047* (Issue 06).

Pollution Control Department (PCD). (2019). *Booklet on Thailand State of Pollution 2018(*Report) (Issue 06). http://www.pcd.go.th/file/BookletonThailandStateof Pollution 2018.pdf

Yang, Q., Li, T., Shen, H., L. Z. (n.d.). *Title: The relationships between $PM_{2.5}$ and meteorological factors in China: Seasonal and regional variations*.(pp.1–37).

Samermit, R. (2020). *Applications of hourly aerosol optical depth from the Himawari-8 satellite to estimate the $PM_{2.5}$ concentration in Chiang Mai province*. (Master Thesis No. EV-20-10, Asian Institute of Technology, 2020). Bangkok: Asian Institute of Technology.

Xiaoli, W., Ni-Bin, C., Kaixu, B., & Wei G. (2020) Satellite remote sensing of aerosol optical depth: advances, challenges, and perspectives, *Critical Reviews in Environmental Science and Technology*, 50(16). 1640-1725. https://doi.org/ 10.1080/10643389.2019.1665944

She, L., Zhang, H. K., Li, Z., de Leeuw, G., & Huang, B. (2020). Himawari-8 aerosol optical depth (Aod) retrieval using a deep neural network trained using aeronet observations. *Remote Sensing*, *12*(24), 1–20. https://doi.org/10.3390/rs12244125

Sipelgas, L. (2016). *Application of Satellite Data for Monitoring the Marine Environment*. AIT (Master RSPR No. JUTUK-16-01, Asian Institute of Technology, 2020). Bangkok: Asian Institute of Technology.

Xiao, Q., Wang, Y., Chang, H. H., Meng, X., Geng, G., Lyapustin, A., & Liu, Y. (2017). Full-coverage high-resolution daily $PM_{2.5}$ estimation using MAIAC AOD in the Yangtze River Delta of China. *Remote Sensing of Environment*, *199*, 437–446. https://doi.org/10.1016/j.rse.2017.07.023

Yamashita, K. (2018). Assimilation of Himawari-8 Atmospheric MotionVectors into the Numerical Weather Prediction Systems of the Japan Meteorological Agency. The 97th AMS Annual meeting.